CD33^{KO}-CD33-mesothelin loop CAR design avoids fratricide and improves efficacy of iNK cells against acute myeloid leukemia

Yao Wang[1†], Xiujuan Zheng[1,2,3,4†], Zhiqian Wang[2,3,4], Ziyun Xiao[2,3,4], Yunqing Lin[2,3,4], Fan Zhang[2,3,4], Yanhong Liu[2,3], Pengcheng Liu[2,3,4], Qitong Weng[2,3], Leqiang Zhang[2,3,4], Chengxiang Xia[3], Dehao Huang[3], Lijuan Liu[2,3], Yanping Zhu[2,3], Qi Zhang[2,3], Hanmeng Qi[3], Yi Chen[3], Yiyuan Shen[3], Chenyuan Zhang[2,3,4], Jiacheng Xu[2,3,4], Yaoqin Zhao[2,3,4], Jiaxin Wu[2,3,4], Tongjie Wang[2,3], Mengyun Zhang[2,3], Minming Li[5], Wenbin Qian[6], Aibin Liang[7], Xin Du[5], Wenyu Yang[8], Qi Chen[9], Xiaofan Zhu[8], Fangxiao Hu[3*], Jinyong Wang[1,2,3,4*]

[1]Guangzhou Institutes of Biomedicine and Health, Chinese Academy of Sciences, Guangzhou 510530, China

[2]State Key Laboratory of Organ Regeneration and Reconstruction, Institute of Zoology, Chinese Academy of Sciences, Beijing 100101, China

[3]Beijing Institute for Stem Cell and Regenerative Medicine, Beijing 100101, China

[4]University of Chinese Academy of Sciences, Beijing 100049, China

[5]Department of Hematology, Guangdong Provincial People's Hospital, Guangdong Academy of Medical Sciences, Guangzhou 510080, China

[6]Department of Hematology, the Second Affiliated Hospital, Zhejiang University School of Medicine, Hangzhou 310009, China

[7]Department of Hematology, Tongji Hospital of Tongji University, Shanghai 200065, China

[8]State Key Laboratory of Experimental Hematology, National Clinical Research Center for Blood Diseases, Haihe Laboratory of Cell Ecosystem, Institute of Hematology & Blood Diseases Hospital, Chinese Academy of Medical Science & Peking Union Medical College, Tianjin 300020, China

[9]Center for cell lineage and development, CAS Key Laboratory of Regenerative Biology, Guangdong Provincial Key Laboratory of Stem Cell and Regenerative Medicine, GIBH-HKU Guangdong-Hong Kong Stem Cell and Regenerative Medicine Research Centre, GIBH-CUHK Joint Research Laboratory on Stem Cell and Regenerative Medicine, Guangzhou Institutes of Biomedicine and Health, Chinese Academy of Sciences, Guangzhou, 510530, China.

† These authors contributed equally: Yao Wang, Xiujuan Zheng.

*Correspondence: Fangxiao Hu (hufangxiao@biscrm.ac.cn), Jinyong Wang (wangjinyong@ioz.ac.cn)

One Sentence Summary: Pluripotent stem cell-derived $CD33^{KO}$-LOOP CAR-iNK cells avoid fratricide and demonstrate superior cytotoxicity against $CD33^{+}MSLN^{+}$ leukemia cells.

Abstract

Acute myeloid leukemia (AML) patients are often older, which brings challenges of endurance and persistent efficacy of autologous CAR-T cell therapies. Allogenic CAR-NK cell therapies may offer reduced toxicities and enhanced anti-leukemic potential against AML. In this study, we designed a novel CD33-mesothelin loop CAR (Loop CAR) and evaluated its anti-tumor efficacy in human umbilical cord blood-derived NK (UCB-NK) cells and human pluripotent stem cell-derived NK (hPSC-iNK) cells. The Loop CAR exhibited superior cytotoxicity against dual-antigen-positive tumor cell lines and primary AML cells. To further avoid fratricide caused by endogenous CD33 expression in NK cells, we established a hPSC-derived cell line via knockout of CD33 gene ($CD33^{KO}$) and engineered Loop CAR. Rather than enforced expression of exogenous CD16, we generated abundant mature $CD33^{KO}$-Loop CAR-iNK cells highly expressing endogenous CD16 via an organoid induction approach. This innovative strategy effectively mitigated NK cell fratricide and significantly enhanced CD33 and mesothelin-mediated specific cytotoxicity. Moreover, the $CD33^{KO}$-Loop CAR-iNK cells demonstrated superior tumor-killing activity in AML xenograft mice and significantly prolonged survival. hPSC-derived $CD33^{KO}$-Loop CAR-iNK cells possess unique advantages and translational potential for treating AML.

52 **INTRODUCTION**

53 Acute myeloid leukemia (AML) is an aggressive hematologic malignancy that demands urgent
54 therapy (*1*). As new therapeutic targets are being identified, significant efforts have highlighted
55 mesothelin (MSLN) as a promising target in AML. The MSLN is expressed in 36% of pediatric
56 AML cases and 14% of adult AML cases, with 76% of MSLN-positive ($MSLN^+$) patients
57 retaining MSLN expression at relapse. Furthermore, 4% of MSLN-negative ($MSLN^-$) AML
58 patients acquire MSLN expression upon relapse (*2-4*). Preclinical data suggest that MSLN
59 chimeric antigen receptor (CAR)-T cells effectively eliminate $MSLN^+$ AML cells in xenograft
60 models (*5*). Therefore, MSLN is a promising target for AML immunotherapy.

61 Natural killer (NK) cells have demonstrated considerable potential in enhancing outcomes for
62 AML treatment, particularly in the context of hematopoietic stem cell transplantation (*6*). The
63 adoptive transfer of NK cells for AML therapy has been widely investigated in clinical settings
64 (*7*). CAR-NK cells, which combine the target killing ability of CAR technology with the innate
65 nonspecific cytotoxicity of NK cells, have shown promising results for tumor treatment (*8, 9*).
66 CD33 CAR-NK cells, in particular, have been tested in relapsed/refractory AML therapies,
67 with clinical data demonstrating their efficacy and safety (*10*). Additionally, pluripotent stem
68 cell (PSC)-derived NK or CAR-NK cells have shown therapeutic potential in both preclinical
69 and clinical settings for AML (*11, 12*). PSC-derived NK (iNK) cells provide a homogeneous
70 alternative to NK cells isolated from human tissues (*11, 13, 14*).

71 Despite these advancements, challenges remain in CAR immune cell therapy, such as tumor
72 antigen escape, on-target off-tumor toxicity, and unintended fratricide due to the shared
73 expression of target antigens between CAR immune cells and tumor cells (*15-17*). To overcome
74 these issues, dual-targeting CARs have been designed to simultaneously target two antigens
75 expressed on tumor cells (*18, 19*). Inactivation of the target antigen in the CAR-engineered
76 immune cells, or in healthy tissue cells, can mitigate fratricide and spare normal tissues. For

example, the disruption of CD7 in CD7 CAR-T cells prevents fratricide and allows for the expansion of these cells (*20*). Similarly, genetic inactivation of CD33 in hematopoietic stem cells enables CD33-deficient hematopoiesis to avoid the killing of CD33 CAR-T cells (*21*). Since CD33 is also expressed on NK cells, CD33 CAR-NK cells face similar fratricidal challenges, which can hinder their expansion (*17, 22*). Human umbilical cord blood NK (UCB-NK) cells, which exhibit a 1.4%-25.5% CD33 expression range in their resting state, show reduced cytotoxicity against K562 cells (*23*). Moreover, NK cells upregulate CD33 expression levels to nearly 50% during *in vitro* expansion (*17*).

In this study, we designed a bivalent loop CAR targeting both CD33 and MSLN antigens (CD33-MSLN loop CAR, denoted as Loop CAR). We engineered this Loop CAR into UCB-NK cells and hPSCs to generate Loop CAR-NK and Loop CAR-iNK cells. Both Loop CAR-NK and Loop CAR-iNK cells exhibited superior cytotoxicity against tumor cells expressing CD33 and MSLN antigens, including AML cell lines and patient-derived tumor cells. Transcriptomic analysis confirmed that the Loop CAR enhanced NK cell cytotoxicity. Additionally, we generated a CD33 gene knockout ($CD33^{KO}$) hPSC line expressing the Loop CAR ($CD33^{KO}$-Loop CAR-hPSCs) and successfully produced $CD33^{KO}$-Loop CAR-iNK cells. These $CD33^{KO}$-Loop CAR-iNK cells exhibited enhanced expansion and anti-tumor efficacy *in vitro* and effectively suppressed tumor progression in xenograft AML models. Our findings highlight the clinical potential of Loop CAR-NK and Loop CAR-iNK cells for the treatment of $CD33^{+}MSLN^{+}$ AML.

RESULTS

CD33-MSLN loop CAR-NK cells exhibit superior cytotoxicity against CD33- and MSLN-positive tumor cells

To enhance the efficacy of NK cells targeting mesothelin (MSLN)-expressing acute myeloid leukemia (AML), we employed a bivalent loop CAR strategy, designing a dual-target CAR

102 targeting both CD33 and MSLN. Specifically, the variable light (V_L) and heavy (V_H) chains of
103 anti-CD33 single-chain variable fragment (CD33 scFv) and anti-MSLN scFv (MSLN scFv),
104 the $(G_4S)_3$ linker (Linker 3), and the Whitlow linker (*24*) were sequentially fused to create a
105 bivalent scFv construct (CD33 V_L-linker 3-MSLN V_H-whitlow linker-MSLN V_L-linker 3-
106 CD33 V_H, CD33-MSLN loop). The CD33-MSLN loop scFv was then linked to the CD8α hinge,
107 the CD8 transmembrane domain (TMD), and the CD3 ζ signaling domain (SD) to construct
108 the final CD33-MSLN loop CAR (denoted as Loop CAR). We applied the MSLN CAR and
109 CD33 CAR as controls (**Fig. 1A**). To assess the potential of Loop CAR in enhancing tumor-
110 killing activity in NK cells, we first incorporated the Loop CAR element into the SFG vector,
111 followed by retroviral packaging as previously reported (*25*). After T-cell depletion, umbilical
112 cord blood NK (UCB-NK) cells were activated using K562-mbIL-21 feeder cells for 6 days,
113 followed by transduction with Loop CAR retroviral particles (MOI = 5). The transduced cells
114 were then expanded for 4 days in the presence of K562-mbIL-21 feeder cells (**Fig. 1B** and **fig.**
115 **S1A**). The proportion of Loop CAR^+ NK cells ($CD56^+$CD33 CAR^+MSLN CAR^+) reached 43.4%
116 two days after transduction, while control groups, including EGFP-NK, CD33 CAR-NK, and
117 MSLN CAR-NK, achieved transduction rates of 48.2%, 55.6%, and 52.1%, respectively (**Fig.**
118 **1C**). Loop CAR-NK cells showed comparable expression of typical NK cell activating and
119 inhibitory receptors, as well as cytotoxic granules, to the control groups (**fig. S1B**).
120 We next evaluated the cytotoxicity of Loop CAR-NK cells by sorting CAR^+ NK cells and
121 coculturing them with Nomo-1 ($CD33^+MSLN^+$), AGS ($CD33^-MSLN^+$), or HL-60
122 ($CD33^+MSLN^-$) tumor cells (**Fig. 1**, **D** and **E**, **fig. S1C**). Loop CAR-NK cells exhibited
123 significantly superior cytotoxicity against Nomo-1 cells compared to EGFP-NK, CD33 CAR-
124 NK, and MSLN CAR-NK cells across all effector-to-target (E:T) ratios (E:T = 0.2:1, 0.4:1,
125 0.8:1, 1.6:1) (**Fig. 1F**). In addition, Loop CAR-NK cells also demonstrated potent killing
126 activity against MSLN- or CD33-expressing tumor cells, such as AGS ($CD33^-MSLN^+$) and

127 HL-60 ($CD33^+MSLN^-$), with cytotoxicity comparable to MSLN CAR-NK or CD33 CAR-NK
128 cells (**Fig. 1**, **G** and **H**). Mechanistically, Loop CAR-NK cells exhibited the highest expression
129 of CD107a, a marker associated with NK cell functional activity, when cocultured with Nomo-
130 1 cells (**fig. S1**, **D-F**). Furthermore, Loop CAR molecules accumulated at the immunological
131 synapse (IS) formed between Loop CAR-NK cells and Nomo-1 cells, confirming that the Loop
132 CAR participates in IS formation in a CD33-MSLN-dependent manner (**Fig. 1I**). Notably,
133 Loop CAR-NK cells also demonstrated superior cytotoxicity against primary AML cells
134 expressing both CD33 and MSLN. Mononuclear cells (MNCs) were isolated from the bone
135 marrow (BM) or peripheral blood (PB) of three AML patients (**Fig. 1J**). All three patients'
136 MNCs expressed CD33 (Patient #1: 87.5%, Patient #2: 95.6%, Patient #3: 98.0%) and MSLN
137 (Patient #1: 41.3%, Patient #2: 23.5%, Patient #3: 57.8%) (**Fig. 1K**). The expression of MSLN
138 was further confirmed by qPCR, which showed consistency with the protein expression levels
139 (**Fig. 1L** and **table S1**). Loop CAR-NK cells (Effectors, E) were cocultured with these primary
140 AML cells (Targets, T) for 20 hours at various E:T ratios (0:1, 0.5:1, 1:1, 2:1, and 5:1) (**Fig.**
141 **1M**). Loop CAR-NK cells exhibited significantly higher cytotoxicity against all patient-
142 derived targets compared to CD33 CAR-NK and MSLN CAR-NK cells. In addition, both
143 CD33 CAR-NK and MSLN CAR-NK cells killed more targets than EGFP-NK cells (**Fig. 1**,
144 **N-P**). Collectively, these data demonstrate that Loop CAR-NK cells exhibit superior specific
145 cytotoxicity against tumor cells expressing both CD33 and MSLN compared to CD33 CAR-
146 NK or MSLN CAR-NK cells.

147 **Loop CAR-NK cells exhibit a more pronounced activation status after incubation with**
148 **Nomo-1 cells**

149 To investigate the superior cytotoxicity of Loop CAR-NK cells, we performed single-cell RNA
150 sequencing (scRNA-seq) on sorted Loop CAR-NK cells after incubation with Nomo-1 cells
151 for 72 hours (**Fig. 2A**). UMAP analysis revealed that the transcriptional profiles of Loop CAR-

152 NK cells were similar to those of CD33 CAR-NK or MSLN CAR-NK cells. However, all CAR-
153 NK cells exhibited distinct transcriptional profiles compared to EGFP-NK cells (**Fig. 2B**). We
154 further examined the differentially expressed genes (DEGs) between Loop CAR-NK cells and
155 CD33 CAR-NK or MSLN CAR-NK cells. Gene Ontology (GO) enrichment analysis indicated
156 that genes upregulated in Loop CAR-NK cells relative to MSLN CAR-NK cells were primarily
157 involved in cell division, positive regulation of the Fc receptor-mediated stimulatory signaling
158 pathway, and positive regulation of the RIG-1 signaling pathway (**Fig. 2C** and **fig. S2**, **A** and
159 **B**). Similarly, genes upregulated in Loop CAR-NK cells compared to CD33 CAR-NK cells
160 were enriched in lymphoid cell differentiation, positive regulation of the RIG-1 signaling
161 pathway, and formation of immunological synapses. (**Fig 2D** and **fig. S2**, **C** and **D**). Among the
162 activation-related genes, several hallmarks of NK cell activation and cytotoxic function,
163 including *CD244*, *SLAMF7*, and *ITGAL* (LFA-1), were upregulated (*26-28*). Additionally,
164 genes involved in the RIG-I signaling pathway, such as *ANKRD17*, *PUM1*, and *PUM2* (*29, 30*),
165 and those associated with immunological synapse (IS) formation, including *NCAM1*, *PTK2B*,
166 and *DOCK8* (*31-34*), were also significantly elevated (**Fig. 2**, **E-G**). These findings suggest
167 that Loop CAR-NK cells exhibit enhanced activation following incubation with Nomo-1 cells,
168 which likely contributes to their superior cytotoxicity compared to CD33 CAR-NK or MSLN
169 CAR-NK cells.

170 **The fratricide of Loop CAR-NK and Loop CAR-iNK cells precludes their expansion**

171 The expansion ability of CD33 CAR-NK cells has been impaired due to fratricide mediated by
172 the CD33 CAR, as $CD33^+$ NK cells are eliminated by CAR-expressing NK cells (*17*). Here,
173 the expression of CD33 in UCB-derived Loop CAR-NK cells and hPSC-derived Loop CAR-
174 iNK cells also led to fratricide. In expanded UCB-NK cells, the expression of CD33 was
175 observed at 26.9% (**Fig. 3A)**. To assess fratricide, we sorted $CD33^-$ and $CD33^+$ NK cells as
176 targets and co-incubated them with Loop CAR-NK cells (**Fig. 3**, **B** and **C)**. As expected, Loop

177 CAR-NK cells exhibited specific cytotoxicity against $CD33^+$ NK cells at the indicated effector-
178 to-target (E:T) ratios, while no cytotoxicity was observed against $CD33^-$ NK cells (**Fig. 3D).**
179 We then sorted an equal number of EGFP-NK and Loop CAR-NK cells and cultured them
180 consecutively without K562-mbIL-21 stimulation. Over a 12-day period, the number of Loop
181 CAR-NK cells was lower than EGFP-NK cells, and the gap gradually widened, confirming
182 that fratricide impaired the expansion of Loop CAR-NK cells (**Fig. 3E)**. In our previous work,
183 we established a method for inducing iNK and CAR-iNK cells from pluripotent stem cells (*11,*
184 *35*). Here, we generated a Loop CAR-expressing hPSC line (Loop CAR-hPSCs) and then
185 conducted the induction of Loop CAR-iNK cells (**Fig. 3F**). Briefly, Loop CAR-hPSCs were
186 induced for two days to differentiate into Loop CAR-expressing lateral plate mesoderm cells
187 (Loop CAR-iLPM), which were then combined with OP9 cells to form organoid aggregates.
188 After 25 days of induction, Loop CAR-iNK cells were generated (**Fig. 3G**). The resulting Loop
189 CAR-iNK cells expressed similar levels of CD56 and CD16 as iNK cells, with 78.6% of the
190 cells expressing the Loop CAR (**Fig. 3H**). Moreover, Loop CAR-iNK cells showed comparable
191 expression of typical NK cell cytotoxic effectors to the iNK cells (**fig. S3A**). Notably, the CD33
192 expression level in iNK cells was 69.7%, which was significantly higher than that observed in
193 tissue-derived NK cells (**Fig. 3I**). Next, we sorted $CD33^-$ and $CD33^+$ iNK cells and co-
194 incubated them with Loop CAR-iNK cells (**Fig. 3**, **J** and **K**). The Loop CAR-iNK cells showed
195 significant cytotoxicity against $CD33^+$ iNK cells compared to $CD33^-$ iNK cells (**Fig. 3L**). As
196 observed with the Loop CAR-NK cells, the number of Loop CAR-iNK cells gradually declined
197 during a 12-day expansion period, reinforcing that fratricide significantly impaired the
198 expansion of Loop CAR-iNK cells (**Fig. 3M**). Taken together, the expression of CD33 in Loop
199 CAR-NK and Loop CAR-iNK cells led to fratricide, which precluded their expansion.

200 **CD33 inactivation in iNK cells preserves their broad-spectrum cytotoxicity and facilitates**
201 **the expansion of Loop CAR-iNK cells**

202 To address the fratricide caused by CD33 expression in Loop CAR-iNK cells, we generated a
203 CD33 gene knockout hPSC ($CD33^{KO}$-hPSC) line using the CRISPR/Cas12i system. Vectors
204 carrying Cas12i, sgRNA1 (5'-TTCAGAAGTGGCCGCAAGGGAAG-3'), sgRNA2 (5'-
205 TTGCTAGTCATCCCCAAATATCC-3'), and a neomycin resistance gene were transduced
206 into hPSCs (**Fig. 4A**). Following neomycin selection, single clones were isolated and
207 genotyped using four pairs of PCR primers (**fig. S4**, **A** and **B**). Ultimately, we identified a
208 $CD33^{KO}$-hPSC clone with the deletion of exon 3 and exon 4 in one allele of CD33 and the
209 insertion of a loxp-NeoR-loxp sequence in the other (**Fig. 4B** and **fig. S4**, **C** and **D**).
210 Subsequently, $CD33^{KO}$-hPSCs successfully generated CD33-deficient iNK cells ($CD33^{KO}$-iNK)
211 with immunophenotype similar to iNK cells (**Fig. 4C**). Moreover, the yields of $CD33^{KO}$-iNK
212 cells were comparable to those of iNK cells (**Fig. 4D**). Importantly, $CD33^{KO}$-iNK cells
213 exhibited cytotoxicity against K562 cells equivalent to that of iNK cells, demonstrating that
214 the loss of CD33 did not compromise their broad-spectrum cytotoxicity (**Fig. 4E**). We then
215 introduced the Loop CAR into $CD33^{KO}$-hPSCs to establish the $CD33^{KO}$-Loop CAR-hPSC line.
216 As anticipated, these cells successfully differentiated into $CD33^{KO}$-Loop CAR-iNK cells,
217 which exhibited expression levels of CD56 and CD16 comparable to those of iNK cells, with
218 a CAR expression rate of 89.3% (**Fig. 4**, **F** and **G**). Furthermore, the expression of typical
219 activating and inhibitory receptors, as well as cytotoxic granules, was consistent with that of
220 iNK cells (**fig. S4E**). Most notably, $CD33^{KO}$-Loop CAR-iNK cells demonstrated a similar
221 expansion capacity to that of iNK cells, indicating that CD33 disruption effectively resolved
222 the fratricide issue and restored the proliferation of Loop CAR-iNK cells **(Fig. 4H)**. In
223 conclusion, we successfully mitigated the fratricide issue in Loop CAR-iNK cells by knocking
224 out CD33 in hPSCs, thereby preserving their broad-spectrum cytotoxicity and restoring their
225 expansion.

226 **Genetic disruption of CD33 in Loop CAR-iNK cells enhances their specific cytotoxicity**

227 To evaluate the specific cytotoxicity of $CD33^{KO}$-Loop CAR-iNK cells, we incubated them with
228 Nomo-1 cells or MSLN-expressing HL-60 cells ($MSLN^{+}$ HL-60) (**Fig. 5**, **A** and **B**). Notably,
229 $CD33^{KO}$-Loop CAR-iNK cells exhibited significantly enhanced cytotoxicity compared to Loop
230 CAR-iNK cells, suggesting that fratricide in the latter compromised their specific cytotoxicity
231 (**Fig. 5**, **C** and **D**). To further evaluate the durability of the cytotoxic response, we performed
232 serial killing assays by analyzing the cytotoxicity of $CD33^{KO}$-Loop CAR-iNK cells (**Fig. 5E**).
233 Compared to Loop CAR-iNK cells, $CD33^{KO}$-Loop CAR-iNK cells consistently demonstrated
234 superior specific cytotoxicity against Nomo-1 cells in each round killing assay (**Fig. 5F**).
235 Additionally, we assessed the expression levels of key effector molecules, including TNF-α,
236 IFN-γ, and CD107a, in $CD33^{KO}$-Loop CAR-iNK cells following incubation with Nomo-1 and
237 $MSLN^{+}$ HL-60 cells. The results revealed that $CD33^{KO}$-Loop CAR-iNK cells expressed
238 significantly higher levels of these molecules compared to Loop CAR-iNK cells, further
239 corroborating their enhanced effector function (**Fig. 5**, **G-O**). Collectively, these findings
240 underscore the critical role of CD33 disruption in restoring and strengthening the specific
241 cytotoxicity of Loop CAR-iNK cells, demonstrating its importance in overcoming fratricide-
242 induced functional impairments.

243 **$CD33^{KO}$-Loop CAR-iNK cells effectively suppress AML tumor development in xenograft**
244 **animals**

245 To further evaluate the anti-tumor efficacy of $CD33^{KO}$-Loop CAR-iNK cells, we employed an
246 AML xenograft mouse model, using iNK cells as control effectors (**Fig. 6A**). $MSLN^{+}$ HL-60
247 cells were intravenously injected into NCG mice (5×10^5 cells/mouse) on day -1 to establish
248 the AML xenograft models. Mice with comparable tumor burdens were randomly assigned to
249 three groups (Tumor only, iNK, and $CD33^{KO}$-Loop CAR-iNK). $CD33^{KO}$-Loop CAR-iNK cells
250 were administered intravenously at a dose of 1×10^7 cells/mouse on days 0 and 3 (**Fig. 6B**).
251 Tumor progression was monitored weekly using bioluminescence imaging (BLI). The results

252 showed that the tumor burden in mice treated with $CD33^{KO}$-Loop CAR-iNK cells was
253 significantly lower than in those treated with iNK cells, demonstrating the potent anti-tumor
254 activity of $CD33^{KO}$-Loop CAR-iNK cells (**Fig. 6**, **C** and **D**). Moreover, the enhanced tumor
255 suppression translated into a significant survival benefit, with $CD33^{KO}$-Loop CAR-iNK-treated
256 mice achieving a median survival of 42 days, compared to shorter survival in the control groups
257 (**Fig. 6E**). Collectively, these findings demonstrate that $CD33^{KO}$-Loop CAR-iNK cells
258 effectively eliminate AML tumor cells *in vivo* and prolong the survival of xenograft models,
259 underscoring their therapeutic potential for clinical application.

260 **DISCUSSION**

261 The dual CAR strategy is an effective approach to prevent tumor escape caused by antigen
262 heterogeneity or loss. Bivalent CAR, one CAR containing two scFvs, which can result in higher
263 transduction efficiency than bicistronic CAR, two single-targeted CARs. Bivalent CAR can be
264 categorized into tandem CAR and loop CAR (*36*). Previous studies have reported that loop
265 CAR exhibited superior anti-tumor potency than tandem CAR (*37, 38*). In this study, we
266 developed a bivalent loop CAR targeting CD33 and mesothelin (MSLN) (CD33-MSLN loop
267 CAR, denoted as Loop CAR). When the Loop CAR expression cassette was introduced into
268 umbilical cord blood NK (UCB-NK) cells, the resulting Loop CAR-NK cells exhibited superior
269 cytotoxicity against CD33 and MSLN-expressing tumor cells, including Nomo-1 and primary
270 $CD33^{+}MSLN^{+}$ AML cells. Furthermore, Loop CAR-NK cells demonstrated comparable
271 cytotoxicity against $CD33^{+}MSLN^{-}$ and $CD33^{-}MSLN^{+}$ tumor cells compared to CD33 CAR-
272 NK and MSLN CAR-NK cells. The accumulation of Loop CAR proteins at the immunological
273 synapse between Loop CAR-NK cells and Nomo-1 cells likely contributes to their enhanced
274 specific cytotoxicity (*39, 40*). Additionally, Nomo-1 cells stimulated Loop CAR-NK cells to
275 express higher levels of CD107a, a membrane protein associated with NK cell cytotoxic
276 activity (*41*). Transcriptome analysis revealed that Loop CAR-NK cells exhibited upregulated

signaling pathways related to cell division and activation after incubation with Nomo-1 cells. Genes such as *NCAM1*, *PTK2B*, and *DOCK8*, which are involved in immunological synapse formation and cytotoxic function, were significantly upregulated (*31-34, 42*).

Consistent with the previous report (*23*), a fraction of UCB-NK cells naturally express CD33. Our findings confirmed that hPSC-derived iNK cells exhibit even higher levels of CD33 expression compared to UCB-NK cells. This led to fratricide in both Loop CAR-NK and Loop CAR-iNK cells, ultimately impairing their expansion. Similar fratricide-induced expansion impairments have been previously reported in human tissue-derived CD33 CAR-NK cells (*17*), highlighting the necessity of addressing this challenge. To overcome the fratricide issue, we genetically disrupted CD33 in hPSCs ($CD33^{KO}$-hPSCs) using CRISPR/Cas technology. Previous studies have shown that CD33 knockout in hematopoietic stem cells allows for the development of a functional hematopoietic system without impairing differentiation potential (*21*). Our results demonstrated that $CD33^{KO}$-hPSCs successfully differentiated into iNK cells without affecting their induction efficiency or anti-tumor activity. Although CD33 has been considered an inhibitory receptor due to its cytoplasmic tyrosine-based inhibitory motifs (ITIMs) (*43*). We observed no significant differences in cytotoxicity against K562 cells between $CD33^{KO}$-iNK and iNK cells.

As expected, $CD33^{KO}$-Loop CAR-hPSCs efficiently generated $CD33^{KO}$-Loop CAR-iNK cells. The elimination of CD33 expression successfully prevented fratricide and restored the expansion capacity of Loop CAR-iNK cells. Interestingly, $CD33^{KO}$-Loop CAR-iNK cells demonstrated superior specific cytotoxicity against Nomo-1 and $MSLN^{+}$ HL-60 cells compared to Loop CAR-iNK cells, indicating that fratricide in the latter not only impaired their expansion but also reduced their specific cytotoxicity. Moreover, $CD33^{KO}$-Loop CAR-iNK cells significantly suppressed tumor progression and prolonged the survival of AML xenograft mice. We used $MSLN^{+}$ HL-60 cells, an M2 subtype of acute myeloid leukemia (AML), to

construct the tumor models, as these cells exhibit high tumorigenic potential *in vivo*. Additionally, we attempted to use Nomo-1 cells, an M5a subtype of acute monocytic leukemia, to establish a tumor model. However, the tumorigenic efficiency was suboptimal with Nomo-1 cells. Given NK cells' relatively lower genome editing efficiency compared to T cells (*44*), targeting endogenous CD33 at the pluripotent stem cell (PSC) stage represents a more practical approach to avoid potential fratricide. With their amenability to genetic engineering, clonal selection capabilities, and lack of T cell contamination, PSC-derived NK cells hold promise as standardized, off-the-shelf immunotherapy products (*45, 46*).

Despite significant progress in identifying AML-specific antigens as therapeutic targets, challenges remain due to their genomic and phenotypic heterogeneity and overlapping expression with normal hematopoietic cells (*5*). CD33, expressed in over 80% of AML cells, is absent from primitive stem cells and multipotent progenitor cells, making it an attractive target for AML immunotherapy (*47, 48*). Recent clinical data have demonstrated the safety and efficacy of functionally enhanced CD33 CAR-NK cells (*10*). MSLN, a well-established target in solid tumors, is expressed in approximately 36% of pediatric AML cases and 14% of adult AML cases, but is virtually absent in normal hematopoietic cells (*4*). MSLN CAR-T cells can efficiently eliminate MSLN-positive ($MSLN^{+}$) AML cells in xenograft models derived from cell lines and patients (*5*). However, MSLN is actively cleaved from the cell membrane and is not highly expressed in AML cells. Strategies such as small molecules (e.g., INCB7839, GM6001) and immunotoxins (e.g., RG7787, SS1P) have been developed to upregulate MSLN expression and reduce shedding, thereby enhancing its viability as a therapeutic target (*5, 49, 50*). Our findings demonstrated that CD33-MSLN loop CAR-NK cells exhibited superior cytotoxicity against primary AML cells expressing both CD33 and MSLN (23.5%-57.8%). Moreover, $CD33^{KO}$-CD33-MSLN loop CAR-iNK cells displayed robust anti-tumor efficacy both *in vitro* and in xenograft models. These results indicate that the CD33-MSLN loop CAR

design effectively enhances the tumor-killing potential of NK cells and supports the successful development of a dual-targeting CAR strategy. Additionally, by genetically inactivating CD33, we effectively addressed the fratricide issue, further improving the function of CD33-MSLN loop CAR-iNK cells. In conclusion, our study provides compelling preclinical evidence supporting the further evaluation of CD33-MSLN loop CAR-NK and $CD33^{KO}$-CD33-MSLN loop CAR-iNK cells as promising candidates for clinical trials in the treatment of $MSLN^{+}$ AML.

MATERIALS AND METHODS

Study design

The objective of this study was to develop a more efficient therapeutic CAR-NK cell for the treatment of acute myeloid leukemia (AML). This was achieved by designing a bivalent CD33-MSLN loop CAR (Loop CAR) and inactivating CD33, thereby generating Loop CAR-iNK cells that avoid fratricide and effectively target and kill $MSLN^{+}CD33^{+}$ AML cells. The construction of Loop CAR was described in the results. The functionality of the Loop CAR was validated by cloning its expression elements into the SFG vector and employing the RD114 retroviral system in conjunction with umbilical cord blood NK cells to generate Loop CAR-NK cells. The superior *in vitro* cytotoxicity of Loop CAR-NK cells compared to CD33 CAR-NK and MSLN CAR-NK cells was assessed through tumor killing assays against $CD33^{+}MSLN^{+}$ tumor cell lines (Nomo-1 and $MSLN^{+}$ HL-60). Furthermore, the expression of CD107a in CAR-NK cells stimulated by Nomo-1 cells was analyzed to evaluate degranulation capacity. Single-cell RNA sequencing (scRNA-seq) using the 10× Genomics platform further demonstrated the enhanced effector functions of loop CAR-NK cells at the transcriptomic level following co-incubation with Nomo-1 cells.

To extend this strategy, the Loop CAR was introduced into hPSCs to generate Loop CAR-iNK cells. However, functional assays revealed that both Loop CAR-NK and Loop CAR-NK iNK cells exhibited fratricide by targeting $CD33^{+}$ NK cells or iNK cells, leading to limited expansion. To address this challenge, the CRISPR/Cas12i system was employed to generate a CD33 knockout ($CD33^{KO}$) hPSC line. We first confirmed that CD33 disruption did not affect the immunophenotype or cytotoxic function of iNK cells through flow cytometric immunophenotypic analysis and tumor-killing assays against K562 cells. Subsequently, the Loop CAR was introduced into the $CD33^{KO}$-hPSCs to produce $CD33^{KO}$-Loop CAR-iNK cells. Flow cytometric analysis and *in vitro* expansion experiments confirmed that the loss of CD33

359 did not alter the immunophenotypic characteristics of Loop CAR-iNK cells but significantly
360 enhanced their expansion potential. To validate the improved *in vitro* effector functions of
361 $CD33^{KO}$-Loop CAR-iNK cells, tumor-killing assays and flow cytometry analysis of CD107a
362 expression and effector molecule secretion (IFN-γ and TNF-α) were conducted following
363 stimulation with Nomo-1 and $MSLN^{+}$ HL-60 cells. To assess the *in vivo* anti-tumor efficacy of
364 $CD33^{KO}$-Loop CAR-iNK cells, AML xenograft models were established using $MSLN^{+}$ HL-60
365 cells in NCG mice. Tumor-bearing mice were treated with either iNK or $CD33^{KO}$-Loop CAR-
366 iNK cells, and therapeutic efficacy was monitored through weekly bioluminescence imaging.
367 Blinding was not employed in the experiments. Each experiment was conducted independently
368 on different days using different batches of reagents. Experimental data were repeated to ensure
369 an adequate number of biological replicates. Details regarding sample sizes, replicates, and
370 statistical analyses are provided in the figures, figure legends, and supplementary materials.

371 **Cell culture**

372 Human embryonic kidney (HEK) 293T cells (ATCC) were cultured in Dulbecco's Modified
373 Eagle Medium (DMEM, Gibco) supplemented with 10% fetal bovine serum (FBS,
374 HUANGKE). Human cervical cancer HeLa cells (Procell Life Science & Technology Co., Ltd)
375 were maintained in Minimum Essential Medium α (MEMα, Gibco) with 10% FBS.
376 Mesothelin-expressing ($MSLN^{+}$) AML cell lines, Nomo-1 (COBIOER), and luciferase-
377 expressing Nomo-1 were maintained in RPMI 1640 (Gibco) supplemented with 10% FBS.
378 Human gastric adenocarcinoma AGS cells (Procell Life Science & Technology Co., Ltd) were
379 cultured in Ham's F12 (Gibco) supplemented with 10% FBS. HL-60 (Procell Life Science &
380 Technology Co., Ltd) and luciferase-expressing $MSLN^{+}$ HL-60 ($MSLN^{+}$ HL-60 $luci^{+}$) cells
381 were cultured in Iscove's Modified Dulbecco's Medium (IMDM, Gibco) supplemented with
382 20% FBS. To generate MSLN-expressing HL-60 cell line, the cDNA encoding MSLN was
383 inserted into the PiggyBac expression vector (SBI) to generate a recombinant vector. The

384 MSLN-expressing PiggyBac vector and the transposase expression vector were electroporated
385 into HL-60 cells using Electroporator EX+ (Celetrix). Seven days after electroporation, HL-60
386 cells were sorted for two rounds to establish the MSLN-expressing HL-60 cell line. The PSC
387 line (Q380-ESC) was provided by the National Stem Cell Resource Center, Institute of Zoology,
388 Chinese Academy of Sciences. All hPSCs were kept in Essential 8 Medium (Gibco) on
389 Vitronectin-Recombinant Human Protein (rhVTN-N, Gibco) coated plates. The hPSCs
390 differentiation toward iNK and the related anti-tumor activity assessments of iNK cells in
391 animals were approved by the Biomedical Research Ethics Committee of the Institute of
392 Zoology, Chinese Academy of Sciences.

393 **Generation of CAR constructs and CAR-modified NK cells**

394 The monospecific CAR constructs included a signal peptide (SP), the anti-CD33 or anti-
395 mesothelin (MSLN) single-chain variable fragment (scFv) (*51, 52*), the CD8α hinge domain, a
396 transmembrane domain (TMD) of CD8, and a signaling domain (SD) of CD3ζ. The Loop CAR
397 construct was designed using the same backbone, with the scFv arrangement as follows: CD33
398 (V_L)-MSLN (V_H)-MSLN (V_L)-CD33 (V_H) were fused with the G4S linker and the whitlow
399 linker (*53*). The EGFP coding sequence or CAR constructs were cloned into SFG recombinant
400 retroviral vectors (*54*). Retroviruses carrying the CAR vectors were generated as previously
401 described (*25*). Umbilical cord blood (UCB) units were provided by Guangdong Cord Blood
402 Bank (Guangzhou, China). $CD3^-$ umbilical cord blood mononuclear cells (UCBMCs) were
403 isolated, and activated NK cells were produced as previously described (*25*). On day 0,
404 activated NK cells were transduced with retroviral supernatants at a multiplicity of infection
405 (MOI) of 5, following the Vectofusin-1 (Miltenyi Biotec) based transduction protocol. Infection
406 rates were assessed by flow cytometry on day 2. CAR-NK cells were harvested for use after 4

407 days of expansion. The CAR-NK cells were sorted and expanded for 12 days without
408 stimulation by K562-mbIL-21 cells (Hangzhou Zhongying Biomedical Technology Co., Ltd).

409 **Flow cytometry**

410 Transduced UCB-NK cells were stained with fluorochrome-conjugated antibodies against CD3
411 (UCHT1), CD56 (HCD56) (Biolegend), CD33 scFv, and MSLN scFv (ACROBiosystems) for
412 analysis of CAR expression using a BD LSRFortessa flow cytometer (BD Biosciences). Anti-
413 CD56, anti-CD33 scFv, and anti-MSLN scFv antibodies were used to sort CAR-NK cells using
414 Sony MA900 (SONY). Human anti-CD33 antibody (P67.6, Biolegend) and human anti-MSLN
415 antibody (Abcam) were used to determine the expression levels of CD33 and MSLN in tumor
416 cell lines and primary AML cells. The immunophenotypes of iNK cells were analyzed using
417 antibodies against CD45 (HI30, Biolegend), CD3, CD56, CD16 (3G8, Biolegend), CD33 scFv
418 and MSLN scFv. To evaluate the expression of NK receptors and effector molecules, we used
419 antibodies against CD56, NKp44 (P44-8), NKp30 (P30-15), NKG2D (1D11), CD69 (FN50),
420 CD16, CD319 (162.1), CD226 (11A8), CD96 (NK92.39), CD94 (HP-3D9), NKG2A
421 (S19004C), Perforin (dG9), GzmB (QA18A28) (all from Biolegend), CD33 scFv and MSLN
422 scFv. Cells were resuspended in DAPI (Sigma-Aldrich) or Dulbecco's phosphate-buffered
423 saline (BasalMedia Technologies) for analysis with the BD LSRFortessa cytometer (BD
424 Biosciences). Data were analyzed with FlowJo software (FlowJo_v10.8.1).

425 **Cytotoxicity assays**

426 For cytotoxicity assessment, target cells, labeled with eBioscience™ Cell Proliferation Dye
427 eFluor™ 670 (eFluor 670) (Invitrogen), were co-cultured with NK cells in the indicated
428 effector (E) to target (T) ratios (E:T). Target cell death was quantified using the BD
429 LSRFortessa flow cytometer or BD LSRFortessa X-20 cytometer (BD Biosciences) by

430 measuring the percentage of DAPI$^+$ among eFluor 670-labeled cells. In serial killing assays,
431 iNK cells received three rounds tumor challenge. Round 1: eFluor 670-labeled (eFluor 670$^+$)
432 Nomo-1 cells were mixed with relevant iNK cells and co-incubated for 12 h (E:T = 1:1).
433 Analysis of the cell lysis of eFluor 670$^+$ Nomo-1 cells at 12 h represents the Round 1
434 cytotoxicity of the relevant iNK cells. Round 2: Unlabeled Nomo-1 cells were mixed with
435 relevant iNK cells and co-incubated for 12 h (E:T = 1:1). Equal numbers of eFluor 670-labeled
436 Nomo-1 cells were added and co-incubated for the next 12 h. Analysis of the cell lysis of eFluor
437 670$^+$ Nomo-1 cells at 24 h represents the Round 2 cytotoxicity of the relevant iNK cells. Round
438 3: Unlabeled Nomo-1 cells were mixed with relevant iNK cells (E:T = 1:1). Equal numbers of
439 unlabeled Nomo-1 cells and eFluor 670-labeled Nomo-1 cells were added at 12 h and 24 h
440 respectively. Analysis of the cell lysis of eFluor 670$^+$ Nomo-1 cells at 36 h represents the Round
441 3 cytotoxicity of the relevant iNK cells. Specific cytotoxicity was calculated using the formula:
442 (percentage of specific death – percentage of spontaneous death) / (1 – percentage of
443 spontaneous death) × 100%.

444 **Assessment of CD107a, TNF-α, and IFN-γ by flow cytometry**

445 To evaluate CD107a expression, NK or iNK cells were co-cultured with or without Nomo-1 or
446 MSLN$^+$ HL-60 cells at an E:T ratio of 0.5:1 for 4 h. After incubation, cells were stained with
447 antibodies against CD56, CD107a (H4A3, Biolegend), CD33 scFv, and MSLN scFv. To
448 evaluate TNF-α and IFN-γ expression, iNK cells were co-cultured with or without Nomo-1 or
449 MSLN$^+$ HL-60 cells at an E:T ratio of 0.5:1 for 2 h, followed by adding BFA/Monensin
450 (MULTISCIENCES) for additional 2-h incubation. After incubation, cells were stained with
451 antibodies against CD56, CD33 scFv, and MSLN scFv. FIX &PERM Kit (MULTISCIENCES)
452 was used for fixation and permeabilization, followed by intracellular staining for TNF-α
453 (Biolegend, MAb11) or IFN-γ (Biolegend, 4S.B3). The cells were analyzed with BD

454 LSRFortessa X-20 cytometer (BD Biosciences). Data were analyzed with FlowJo software
455 (FlowJo_v10.8.1).

456 **Immunofluorescence imaging**

457 Immunofluorescence imaging of immune synapses of Loop CAR-NK cells by confocal
458 microscopy as previously described (*55*). Briefly, immune synapses of Loop CAR-NK cells
459 were formed by suspending NK cells at 5×10^6/mL and Nomo-1 target cells at 2.5×10^6/mL.
460 Equal volumes of Loop CAR-NK cell and Nomo-1 target cell suspensions were mixed and
461 incubated to form conjugates. Loop CAR-NK and Nomo-1 cell conjugates were permeabilized
462 using the FIX & PERM kit (MULTISCIENCES) and stained with antibodies against phalloidin
463 (Thermo Fisher Scientific), CD33 scFv, MSLN scFv, pericentrin (Abcam), and perforin
464 (Biolegend). Sequential scanning with a Leica TCS SP8 laser scanning confocal microscope
465 imaged NK cell immune synapses. The images were acquired using LASAF software (Leica).

466 **Quantitative real-time PCR**

467 The *MSLN* transcripts were reverse transcribed into cDNA using HiScript III All-in-One RT
468 SuperMix Perfect for qPCR (Vazyme) and quantified by quantitative real-time PCR using
469 Hieff® qPCR SYBR® Green Master Mix (Yeasen Biotechnology). *GAPDH* was used for
470 normalization. The relative gene expression levels were calculated as $2^{-\Delta Ct}$. All primers used in
471 this study were listed in **table S1**.

472 **Primary samples**

473 Primary AML cells were isolated from AML diagnostic bone marrow or peripheral blood
474 samples obtained from the State Key Laboratory of Experimental Hematology, National
475 Clinical Research Center for Blood Diseases, Institute of Hematology & Blood Diseases

476 Hospital, Chinese Academy of Medical Science & Peking Union Medical College, and
477 Department of Hematology, Guangdong Provincial People's Hospital. Primary AML cells were
478 thawed for immunophenotype analysis of MSLN expression and cultured in IMDM
479 supplemented with 20% FBS, 10 ng/ml GM-CSF (MedChemExpress), 100 U/ml DNase I
480 (Sigma Aldrich), and 50 uM GM6001 (Selleck) (a matrix metalloprotease inhibitor that
481 stabilizes MSLN expression on the cell surface (*5*) for cytotoxicity assays. *In vitro* killing
482 assays were performed as mentioned above. The use of patient samples was carried out by the
483 provisions of the Declaration of Helsinki. All patient samples were collected with patient
484 consent signatures and reviewed and approved by the Ethics Committee of the Hospital for
485 Hematology & Blood Diseases and the Guangdong Provincial People's Hospital, respectively.

486 **Single-cell RNA-sequencing and data analysis**

487 FACS-sorted EGFP-NK ($CD56^+EGFP^+$) and CAR-NK cells ($CD56^+CAR^+$) were activated
488 with eFluor 670 labeled (eFluor 670^+) Nomo-1 cells for 72 h. Fifty thousand cells sorted (eFluor
489 670^- and $CD56^+$) from activated NK populations underwent RNA-sequencing (10× Genomics).
490 Droplet-based scRNA-seq datasets were generated using a Chromium system (10× Genomics,
491 PN120263) following the manufacturer's instructions. The raw data were uploaded to the
492 public database of Genome Sequence Archive (HRA008163). Subsequently, these data sets
493 were aligned and quantified using the CellRanger software package (version 6.0.0) and
494 subjected to Seurat (version 3.2.3) for further analysis. To pass quality control, cells were
495 required to have at least 200 genes detected, less than 7,500 genes detected, and less than 20%
496 of aligned reads mapped to mitochondrial genes. 15,408, 17269, 15273, and 16734 cells from
497 EGFP-NK, CD33 CAR-NK, MSLN CAR-NK, and Loop CAR-NK scRNA-seq datasets that
498 passed quality control were merged and used for downstream analysis. The Unique Molecular
499 Identifier (UMI) value was normalized using Seurat's 'LogNormalize' and 'ScaleData'

methods. The Principal Component Analysis (PCA) used 2,000 highly variable genes (as defined by Seurat), and clustering was performed on the most variable principal components (PCs). The most variable PCs were determined by the Jackstraw method. Then, the 36 most variable PCs were used for clustering and Uniform Manifold Approximation and Projection (UMAP) analysis with resolution 0.2 and other default parameters. The median and dot plots for gene expression were plotted using the Seurat VlnPlot function and the ggplot2 package. Differential expression genes (DEGs) were identified using the neurinoma test with the parameter 'min.pct = 0.25, logfc threshold = 0.25'. Gene ontology (GO) enrichment analysis for DEGs was performed by the clusterProfiler package (version 4.2.2) with BH adjusted cutoff value = 0.05. Box plots of the normalized expression of DEGs were plotted using the ggplot2 package. Volcano plots were plotted using ggplot2 and the ggrepel package.

Regeneration of CAR-iNK cells

CAR-expressing hPSCs were engineered using the piggyBac transposon system, as mentioned above. CAR-iNK cells were regenerated from CAR-transfected hPSCs and harvested for use as previously described (*11*). Briefly, CAR-hPSCs were performed a two-day induction to produce CAR lateral plate mesoderm cells (CAR-iLPM). Then 2×10^4 CAR-iLPM were combined with 5×10^5 OP9 cells to form organoid aggregates and seeded in the transwell (Corning, 3450). Subsequently, the medium was changed every 2-3 days to induce NK cell regeneration. After 25 days of induction, mature CAR-iNK cells were harvested for use.

CRISPR/Cas12i-mediated CD33 knockout in hPSCs

Two sgRNA sequences, sgRNA1 (TTCAGAAGTGGCCGCAAGGGAAG) and sgRNA2 (TTGCTAGTCATCCCCAAATATCC), targeting exon 3 and exon 4 of CD33 respectively, were designed using a web-based guide-RNA designer (http://www.rgenome.net/) and

523 subsequently cloned into the Cas12i expression vector (a gift from Dr. Wei Li of the Institute
524 of Zoology, Chinese Academy of Sciences) (*56*). To create CD33 knockout hPSCs ($CD33^{KO}$-
525 hPSCs), the two Cas12i-sgRNA expression vectors and a donor vector carrying the neomycin
526 resistance gene (NeoR) were co-transfected into hPSCs using electroporation. Five days post-
527 transfection, G418 (InvivoGen) was introduced to select the targeted hPSCs for one week.
528 Following G418 selection, the cells were digested and single cells were seeded into 96-well
529 plates to form single-cell clones. PCR and sequencing were used to verify the mutation sites,
530 thereby establishing CD33 knockout clones.

531 **Genome PCR**

532 Single-cell clones of hPSCs resistant to G418 were harvested for DNA extraction using the
533 TIANamp Genomic DNA kit (TIANGEN). The CD33 locus target sequences were amplified
534 with the 2 × Rapid Taq Master Mix (Vazyme) and the primer pairs depicted in **fig. S4**.

535 **AML xenograft models with CAR-iNK cell treatment**

536 The $MSLN^{+}$ HL-60 $luci^{+}$ cells (5×10^{5} cells/mouse) were injected intravenously into NCG
537 mice (NOD/ShiLtJGpt-*Prkdc*^{em26Cd52}*Il2rg*^{em26Cd22}/Gpt strain, GemPharmatech Co., Ltd.) to
538 establish human AML xenograft models on day -1. On day 0, bioluminescence imaging (BLI,
539 IVIS Spectrum PerkinElmer) was used to quantify the tumor graft burden in each group. After
540 irradiation (1.0 Gy, Rad Source RS2000), the animals were randomly assigned to treatment
541 groups and received an intravenous injection of the equivalent of 1×10^{7} fresh CAR^{+} iNK or
542 unmodified iNK cells. Three days later (day 3), the animals received the second intravenous
543 injection with the same cell count. Tumor aggressiveness was determined weekly by BLI. Mice
544 with a significant tumor burden were humanely euthanized. All animal experiments were

conducted under the Institutional Animal Care and Use Committee (IACUC) of the Institute of Zoology of the Chinese Academy of Sciences (IOZ-2021-182).

Statistical analysis

All quantitative analysis were performed with SPSS (IBM SPSS Statistics 25). The Shapiro-Wilk normality test assessed the normal distribution of the data. Quantitative differences (mean ± SD) between samples were compared using two-tailed Student's t-test, Mann-Whitney U test, one-way ANOVA test, and two-way ANOVA test. The *P values* were two-sided, and $P < 0.05$ was considered statistically significant. Survival curves for tumor-bearing models were plotted using the Kaplan-Meier method and compared to the treatment group using logarithmic rank (Mantel-Cox) tests. Statistical analysis was performed using the GraphPad Prism 9 software.

List of Supplementary Materials

Fig. S1 to S4 for multiple supplementary figures.

Table S1 for multiple supplementary table.

References and Notes

1. H. Kantarjian, G. Borthakur, N. Daver, C. D. DiNardo, G. Issa, E. Jabbour, T. Kadia, K. Sasaki, N. J. Short, M. Yilmaz, F. Ravandi, Current status and research directions in acute myeloid leukemia. *Blood Cancer J* **14**, 163 (2024).
2. D. Steinbach, A. Schramm, A. Eggert, M. Onda, K. Dawczynski, A. Rump, I. Pastan, S. Wittig, N. Pfaffendorf, A. Voigt, F. Zintl, B. Gruhn, Identification of a set of seven genes for the monitoring of minimal residual disease in pediatric acute myeloid leukemia. *Clin Cancer Res* **12**, 2434-2441 (2006).
3. D. Steinbach, M. Onda, A. Voigt, K. Dawczynski, S. Wittig, R. Hassan, B. Gruhn, I. Pastan, Mesothelin, a possible target for immunotherapy, is expressed in primary AML cells. *Eur J Haematol* **79**, 281-286 (2007).
4. A. J. Kaeding, S. P. Barwe, A. Gopalakrishnapillai, R. E. Ries, T. A. Alonzo, R. B. Gerbing, C. Correnti, M. R. Loken, L. E. Broderson, L. Pardo, Q. H. Le, T. Tang, A. R. Leonti, J. L. Smith, C. K. Chou, M. Xu, T. Triche, S. M. Kornblau, E. A. Kolb, K. Tarlock, S. Meshinchi, Mesothelin is a novel cell surface disease marker and potential therapeutic target in acute myeloid leukemia. *Blood Adv* **5**, 2350-2361 (2021).
5. Q. Le, S. Castro, T. Tang, A. M. Loeb, T. Hylkema, C. N. McKay, L. Perkins, S. Srivastava, L. Call, J. Smith, A. Leonti, R. Ries, L. Pardo, M. R. Loken, C. Correnti, S. Fiorenza, C. J. Turtle, S. Riddell, K. Tarlock, S. Meshinchi, Therapeutic Targeting of Mesothelin with Chimeric Antigen Receptor T Cells

in Acute Myeloid Leukemia. *Clin Cancer Res* **27**, 5718-5730 (2021).

6. K. C. Hsu, C. A. Keever-Taylor, A. Wilton, C. Pinto, G. Heller, K. Arkun, R. J. O'Reilly, M. M. Horowitz, B. Dupont, Improved outcome in HLA-identical sibling hematopoietic stem-cell transplantation for acute myelogenous leukemia predicted by KIR and HLA genotypes. *Blood* **105**, 4878-4884 (2005).
7. S. Z. D'Silva, M. Singh, A. S. Pinto, NK cell defects: implication in acute myeloid leukemia. *Front Immunol* **14**, 1112059 (2023).
8. Y. Kaito, Y. Imai, Evolution of natural killer cell-targeted therapy for acute myeloid leukemia. *Int J Hematol* **120**, 34-43 (2024).
9. Y. Masamoto, M. Kurokawa, A key to engineering natural killer cells to attack acute myeloid leukemia. *Haematologica* **109**, 1032-1034 (2024).
10. R. Huang, X. Wang, H. Yan, X. Tan, Y. Ma, M. Wang, X. Han, J. Liu, L. Gao, L. Gao, G. Jing, C. Zhang, Q. Wen, X. Zhang, Safety and efficacy of CD33-targeted CAR-NK cell therapy for relapsed/refractory AML: preclinical evaluation and phase I trial. *Exp Hematol Oncol* **14**, 1 (2025).
11. D. Huang, J. Li, F. Hu, C. Xia, Q. Weng, T. Wang, H. Peng, B. Wu, H. Wu, J. Xiong, Y. Lin, Y. Wang, Q. Zhang, X. Liu, L. Liu, X. Zheng, Y. Geng, X. Du, X. Zhu, L. Wang, J. Hao, J. Wang, Lateral plate mesoderm cell-based organoid system for NK cell regeneration from human pluripotent stem cells. *Cell Discov* **8**, 121 (2022).
12. A. Eckstrom, A. Tyagi, S. Mahmood, L. Wong, B. Valamehr, A. Rao, A. Agrawal, M. Siddiqui, V. L. Battula, FT538, iPSC-derived NK cells, enhance AML cell killing when combined with chemotherapy. *J Cell Mol Med* **29**, e70169 (2025).
13. D. A. Knorr, Z. Ni, D. Hermanson, M. K. Hexum, L. Bendzick, L. J. Cooper, D. A. Lee, D. S. Kaufman, Clinical-scale derivation of natural killer cells from human pluripotent stem cells for cancer therapy. *Stem Cells Transl Med* **2**, 274-283 (2013).
14. Y. Li, D. L. Hermanson, B. S. Moriarity, D. S. Kaufman, Human iPSC-Derived Natural Killer Cells Engineered with Chimeric Antigen Receptors Enhance Anti-tumor Activity. *Cell Stem Cell* **23**, 181-192 e185 (2018).
15. E. J. Orlando, X. Han, C. Tribouley, P. A. Wood, R. J. Leary, M. Riester, J. E. Levine, M. Qayed, S. A. Grupp, M. Boyer, B. De Moerloose, E. R. Nemecek, H. Bittencourt, H. Hiramatsu, J. Buechner, S. M. Davies, M. R. Verneris, K. Nguyen, J. L. Brogdon, H. Bitter, M. Morrissey, P. Pierog, S. Pantano, J. A. Engelman, W. Winckler, Genetic mechanisms of target antigen loss in CAR19 therapy of acute lymphoblastic leukemia. *Nat Med* **24**, 1504-1506 (2018).
16. M. L. Cooper, J. Choi, K. Staser, J. K. Ritchey, J. M. Devenport, K. Eckardt, M. P. Rettig, B. Wang, L. G. Eissenberg, A. Ghobadi, L. N. Gehrs, J. L. Prior, S. Achilefu, C. A. Miller, C. C. Fronick, J. O'Neal, F. Gao, D. M. Weinstock, A. Gutierrez, R. S. Fulton, J. F. DiPersio, An "off-the-shelf" fratricide-resistant CAR-T for the treatment of T cell hematologic malignancies. *Leukemia* **32**, 1970-1983 (2018).
17. M. Hejazi, C. Zhang, S. B. Bennstein, V. Balz, S. B. Reusing, M. Quadflieg, K. Hoerster, S. Heinrichs, H. Hanenberg, S. Oberbeck, M. Nitsche, S. Cramer, R. Pfeifer, P. Oberoi, H. Ruhl, J. Oldenburg, P. Brossart, P. A. Horn, F. Babor, W. S. Wels, J. C. Fischer, N. Moker, M. Uhrberg, CD33 Delineates Two Functionally Distinct NK Cell Populations Divergent in Cytokine Production and Antibody-Mediated Cellular Cytotoxicity. *Front Immunol* **12**, 798087 (2021).
18. C. C. Kloss, M. Condomines, M. Cartellieri, M. Bachmann, M. Sadelain, Combinatorial antigen recognition with balanced signaling promotes selective tumor eradication by engineered T cells. *Nat Biotechnol* **31**, 71-75 (2013).
19. D. Abate-Daga, M. L. Davila, CAR models: next-generation CAR modifications for enhanced T-cell function. *Mol Ther Oncolytics* **3**, 16014 (2016).
20. D. Gomes-Silva, M. Srinivasan, S. Sharma, C. M. Lee, D. L. Wagner, T. H. Davis, R. H. Rouce, G. Bao, M. K. Brenner, M. Mamonkin, CD7-edited T cells expressing a CD7-specific CAR for the therapy of T-cell malignancies. *Blood* **130**, 285-296 (2017).
21. M. Y. Kim, K. R. Yu, S. S. Kenderian, M. Ruella, S. Chen, T. H. Shin, A. A. Aljanahi, D. Schreeder, M. Klichinsky, O. Shestova, M. S. Kozlowski, K. D. Cummins, X. Shan, M. Shestov, A. Bagg, J. J. D.

Morrissette, P. Sekhri, C. R. Lazzarotto, K. R. Calvo, D. B. Kuhns, R. E. Donahue, G. K. Behbehani, S. Q. Tsai, C. E. Dunbar, S. Gill, Genetic Inactivation of CD33 in Hematopoietic Stem Cells to Enable CAR T Cell Immunotherapy for Acute Myeloid Leukemia. *Cell* **173**, 1439-1453 e1419 (2018).

22. N. Albinger, R. Pfeifer, M. Nitsche, S. Mertlitz, J. Campe, K. Stein, H. Kreyenberg, R. Schubert, M. Quadflieg, D. Schneider, M. W. M. Kuhn, O. Penack, C. Zhang, N. Moker, E. Ullrich, Primary CD33-targeting CAR-NK cells for the treatment of acute myeloid leukemia. *Blood Cancer J* **12**, 61 (2022).
23. R. Handgretinger, H. J. Schafer, F. Baur, D. Frank, C. Ottenlinger, H. J. Buhring, D. Niethammer, Expression of an early myelopoietic antigen (CD33) on a subset of human umbilical cord blood-derived natural killer cells. *Immunol Lett* **37**, 223-228 (1993).
24. M. Whitlow, B. A. Bell, S. L. Feng, D. Filpula, K. D. Hardman, S. L. Hubert, M. L. Rollence, J. F. Wood, M. E. Schott, D. E. Milenic, et al., An improved linker for single-chain Fv with reduced aggregation and enhanced proteolytic stability. *Protein Eng* **6**, 989-995 (1993).
25. Y. Wang, J. Li, Z. Wang, Y. Liu, T. Wang, M. Zhang, C. Xia, F. Zhang, D. Huang, L. Zhang, Y. Zhao, L. Liu, Y. Zhu, H. Qi, X. Zhu, W. Qian, F. Hu, J. Wang, Comparison of seven CD19 CAR designs in engineering NK cells for enhancing anti-tumour activity. *Cell Prolif* **57**, e13683 (2024).
26. S. O. Mathew, K. K. Rao, J. R. Kim, N. D. Bambard, P. A. Mathew, Functional role of human NK cell receptor 2B4 (CD244) isoforms. *Eur J Immunol* **39**, 1632-1641 (2009).
27. A. Gutierrez-Guerrero, I. Mancilla-Herrera, J. L. Maravillas-Montero, I. Martinez-Duncker, A. Veillette, M. E. Cruz-Munoz, SLAMF7 selectively favors degranulation to promote cytotoxicity in human NK cells. *Eur J Immunol* **52**, 62-74 (2022).
28. D. F. Barber, M. Faure, E. O. Long, LFA-1 contributes an early signal for NK cell cytotoxicity. *J Immunol* **173**, 3653-3659 (2004).
29. Y. Wang, X. Tong, G. Li, J. Li, M. Deng, X. Ye, Ankrd17 positively regulates RIG-I-like receptor (RLR)-mediated immune signaling. *Eur J Immunol* **42**, 1304-1315 (2012).
30. R. Narita, K. Takahasi, E. Murakami, E. Hirano, S. P. Yamamoto, M. Yoneyama, H. Kato, T. Fujita, A novel function of human Pumilio proteins in cytoplasmic sensing of viral infection. *PLoS Pathog* **10**, e1004417 (2014).
31. J. T. Gunesch, A. L. Dixon, T. A. Ebrahim, M. M. Berrien-Elliott, S. Tatineni, T. Kumar, E. Hegewisch-Solloa, T. A. Fehniger, E. M. Mace, CD56 regulates human NK cell cytotoxicity through Pyk2. *Elife* **9**, (2020).
32. D. Sancho, M. Nieto, M. Llano, J. L. Rodriguez-Fernandez, R. Tejedor, S. Avraham, C. Cabanas, M. Lopez-Botet, F. Sanchez-Madrid, The tyrosine kinase PYK-2/RAFTK regulates natural killer (NK) cell cytotoxic response, and is translocated and activated upon specific target cell recognition and killing. *J Cell Biol* **149**, 1249-1262 (2000).
33. H. Ham, W. Huynh, R. A. Schoon, R. D. Vale, D. D. Billadeau, HkRP3 is a microtubule-binding protein regulating lytic granule clustering and NK cell killing. *J Immunol* **194**, 3984-3996 (2015).
34. H. Ham, S. Guerrier, J. Kim, R. A. Schoon, E. L. Anderson, M. J. Hamann, Z. Lou, D. D. Billadeau, Dedicator of cytokinesis 8 interacts with talin and Wiskott-Aldrich syndrome protein to regulate NK cell cytotoxicity. *J Immunol* **190**, 3661-3669 (2013).
35. Y. Liu, M. Zhang, X. Shen, C. Xia, F. Hu, D. Huang, Q. Weng, Q. Zhang, L. Liu, Y. Zhu, L. Wang, J. Hao, M. Zhang, T. Wang, J. Wang, Mesothelin CAR-engineered NK cells derived from human embryonic stem cells suppress the progression of human ovarian cancer in animals. *Cell Prolif* **57**, e13727 (2024).
36. B. Xie, Z. Li, J. Zhou, W. Wang, Current Status and Perspectives of Dual-Targeting Chimeric Antigen Receptor T-Cell Therapy for the Treatment of Hematological Malignancies. *Cancers (Basel)* **14**, (2022).
37. X. Wang, Z. Dong, D. Awuah, W. C. Chang, W. A. Cheng, V. Vyas, S. C. Cha, A. J. Anderson, T. Zhang, Z. Wang, S. J. Szymura, B. Z. Kuang, M. C. Clark, I. Aldoss, S. J. Forman, L. W. Kwak, H. Qin, CD19/BAFF-R dual-targeted CAR T cells for the treatment of mixed antigen-negative variants of acute lymphoblastic leukemia. *Leukemia* **36**, 1015-1024 (2022).
38. Z. Chen, Y. Liu, N. Chen, H. Xing, Z. Tian, K. Tang, Q. Rao, Y. Xu, Y. Wang, M. Wang, J. Wang, Loop

CD20/CD19 CAR-T cells eradicate B-cell malignancies efficiently. *Sci China Life Sci* **66**, 754-770 (2023).

39. J. S. Orange, K. E. Harris, M. M. Andzelm, M. M. Valter, R. S. Geha, J. L. Strominger, The mature activating natural killer cell immunologic synapse is formed in distinct stages. *Proc Natl Acad Sci U S A* **100**, 14151-14156 (2003).
40. E. Liu, Y. Tong, G. Dotti, H. Shaim, B. Savoldo, M. Mukherjee, J. Orange, X. Wan, X. Lu, A. Reynolds, M. Gagea, P. Banerjee, R. Cai, M. H. Bdaiwi, R. Basar, M. Muftuoglu, L. Li, D. Marin, W. Wierda, M. Keating, R. Champlin, E. Shpall, K. Rezvani, Cord blood NK cells engineered to express IL-15 and a CD19-targeted CAR show long-term persistence and potent antitumor activity. *Leukemia* **32**, 520-531 (2018).
41. G. Alter, J. M. Malenfant, M. Altfeld, CD107a as a functional marker for the identification of natural killer cell activity. *J Immunol Methods* **294**, 15-22 (2004).
42. M. Zhang, M. E. March, W. S. Lane, E. O. Long, A signaling network stimulated by beta2 integrin promotes the polarization of lytic granules in cytotoxic cells. *Sci Signal* **7**, ra96 (2014).
43. T. Ulyanova, J. Blasioli, T. A. Woodford-Thomas, M. L. Thomas, The sialoadhesin CD33 is a myeloid-specific inhibitory receptor. *Eur J Immunol* **29**, 3440-3449 (1999).
44. G. M. Robbins, M. Wang, E. J. Pomeroy, B. S. Moriarity, Nonviral genome engineering of natural killer cells. *Stem Cell Res Ther* **12**, 350 (2021).
45. F. Cichocki, S. J. C. van der Stegen, J. S. Miller, Engineered and banked iPSCs for advanced NK- and T-cell immunotherapies. *Blood* **141**, 846-855 (2023).
46. B. H. Goldenson, P. Hor, D. S. Kaufman, iPSC-Derived Natural Killer Cell Therapies - Expansion and Targeting. *Front Immunol* **13**, 841107 (2022).
47. J. Liu, J. Tong, H. Yang, Targeting CD33 for acute myeloid leukemia therapy. *BMC Cancer* **22**, 24 (2022).
48. N. N. Shah, J. Azzi, B. W. Cooper, A. Deol, J. DiPersio, D. Koura, B. McClune, L. S. Muffly, M. U. Mushtaq, R. Narayan, H. C. Suh, G. Yanik, S. Nath, J. Whangbo, G. Koehne, Phase 1/2 Study of Donor-Derived Anti-CD33 Chimeric Antigen Receptor Expressing T Cells (VCAR33) in Patients with Relapsed or Refractory Acute Myeloid Leukemia after Allogeneic Hematopoietic Cell Transplantation. *Blood* **142**, 4862-4862 (2023).
49. C. Alewine, L. Xiang, T. Yamori, G. Niederfellner, K. Bosslet, I. Pastan, Efficacy of RG7787, a next-generation mesothelin-targeted immunotoxin, against triple-negative breast and gastric cancers. *Mol Cancer Ther* **13**, 2653-2661 (2014).
50. P. Awuah, T. K. Bera, M. Folivi, O. Chertov, I. Pastan, Reduced Shedding of Surface Mesothelin Improves Efficacy of Mesothelin-Targeting Recombinant Immunotoxins. *Mol Cancer Ther* **15**, 1648-1655 (2016).
51. P. R. Hamann, L. M. Hinman, I. Hollander, C. F. Beyer, D. Lindh, R. Holcomb, W. Hallett, H. R. Tsou, J. Upeslacis, D. Shochat, A. Mountain, D. A. Flowers, I. Bernstein, Gemtuzumab ozogamicin, a potent and selective anti-CD33 antibody-calicheamicin conjugate for treatment of acute myeloid leukemia. *Bioconjug Chem* **13**, 47-58 (2002).
52. P. S. Chowdhury, J. L. Viner, R. Beers, I. Pastan, Isolation of a high-affinity stable single-chain Fv specific for mesothelin from DNA-immunized mice by phage display and construction of a recombinant immunotoxin with anti-tumor activity. *Proc Natl Acad Sci U S A* **95**, 669-674 (1998).
53. T. J. Fry, N. N. Shah, R. J. Orentas, M. Stetler-Stevenson, C. M. Yuan, S. Ramakrishna, P. Wolters, S. Martin, C. Delbrook, B. Yates, H. Shalabi, T. J. Fountaine, J. F. Shern, R. G. Majzner, D. F. Stroncek, M. Sabatino, Y. Feng, D. S. Dimitrov, L. Zhang, S. Nguyen, H. Qin, B. Dropulic, D. W. Lee, C. L. Mackall, CD22-targeted CAR T cells induce remission in B-ALL that is naive or resistant to CD19-targeted CAR immunotherapy. *Nat Med* **24**, 20-28 (2018).
54. I. Riviere, K. Brose, R. C. Mulligan, Effects of retroviral vector design on expression of human adenosine deaminase in murine bone marrow transplant recipients engrafted with genetically modified cells. *Proc Natl Acad Sci U S A* **92**, 6733-6737 (1995).
55. K. B. Sanborn, G. D. Rak, A. N. Mentlik, P. P. Banerjee, J. S. Orange, Analysis of the NK cell

immunological synapse. *Methods Mol Biol* **612**, 127-148 (2010).
56. Y. Chen, Y. Hu, X. Wang, S. Luo, N. Yang, Y. Chen, Z. Li, Q. Zhou, W. Li, Synergistic engineering of CRISPR-Cas nucleases enables robust mammalian genome editing. *Innovation (Camb)* **3**, 100264 (2022).

Acknowledgments: We thank the staffs of SPF-grade animal facilities at the Institute of Zoology, Chinese Academy of Sciences for supplying animal care service. **Funding:** This work was supported by grants from the National Key Research and Development Program of China (2021YFA1100701, 2024YFA1108302, 2021YFA1100800), the National Natural Science Foundation of China (82450001, 82470120, 82300132, 32300676, 82350104), and the Noncommunicable Chronic Diseases-National Science and Technology Major Project (2023ZD0501300).

Author contributions

Y.W. and X.J.Z. designed and conducted all experiments, performed data analysis, and wrote the manuscript. Z.Q.W., Z.Y.X., F.Z., Y.H.L., and P.C.L. conducted some experiments and performed data analysis. Y.Q.L. and Q.T.W. performed scRNA-seq and data analysis. L.Q.Z., C.X.X., D.H.H., L.J.L., Y.P.Z., Q.Z., H.M.Q., Y.C., Y.Y.S., C.Y.Z., J.C.X., Y.Q.Z., J.X.W., T.J.W., M.Y.Z., W.Y.Y., and M.M.L. participated in multiple experiments. J.Y.W., X.F.Z., Q.C., X.D., W.B.Q., and A.B.L. discussed the data and manuscript. F.X.H. designed the project, designed and guided all experiments, scrutinized all experimental data, and wrote the manuscript. J.Y.W. revised the manuscript and provided the final approval of the manuscript.

Competing interests

The authors declare that they have no conflict of interest.

Data and materials availability

The scRNA-seq data of EGFP-NK, CD33 CAR-NK, MSLN CAR-NK, and Loop CAR-NK cells stimulated by Nomo-1 cells have been uploaded to the Genome Sequence Archive public database (HRA008163). Other relevant information or data is available from the corresponding

authors upon reasonable request.

Figures

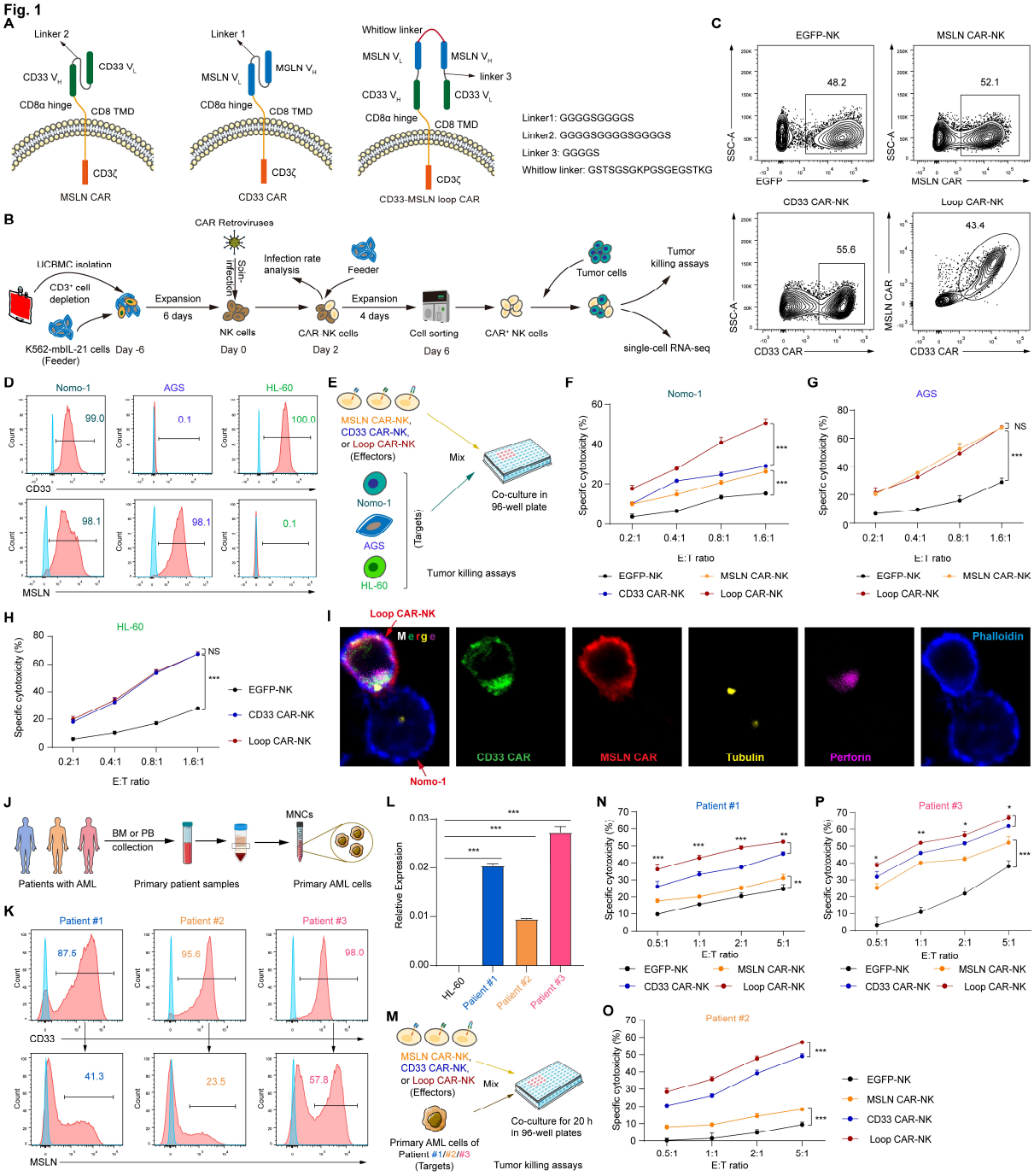

Fig. 1. Development and functional evaluation of Loop CAR-NK cells. (**A**) Schematic diagram of the design of Loop CAR. (**B**) Schematic diagram showing the generation of Loop CAR-NK cells procedures and evaluation their cytotoxicity. (**C**) Flow cytometric analysis of the transduction efficiencies of each group of CAR-NK cells. EGFP virus-infected NK cells were used as control. (**D**) Flow cytometry histograms showing the expression levels of CD33

765 and MSLN in target cell lines, including $CD33^{+}MSLN^{+}$ Nomo-1 AML cells, $CD33^{-}MSLN^{+}$
766 AGS gastric adenocarcinoma cells, and $CD33^{+}MSLN^{-}$ HL-60 AML cells. (**E**) Tumor killing
767 assay design. (**F-H**) Statistics of CAR-NK cells cytotoxicity against Nomo-1 tumor cells (F),
768 AGS cells (G), and HL-60 cells (**H**) at indicated E:T ratios. Nomo-1 cells and HL-60 cells were
769 incubated with effectors for 4 hours (n = 4 per group). AGS cells were incubated with effectors
770 for 6 hours (n = 4 per group). (**I**) Confocal microscopy representative images of immunological
771 synapse formed between loop CAR-NK cells and Nomo-1 cells. The conjugates were stained
772 with antibodies against perforin (Violet), phalloidin-F-actin (Blue), CD33 CAR (Green) and
773 MSLN CAR (Red). (**J**) Schematic diagram showing the collection of peripheral blood or bone
774 marrow cells from patients with AML. (**K**) Flow cytometric analysis of the expression of CD33
775 and MSLN in primary AML cells. (**L**) Real-time quantitative PCR analysis of MSLN transcript
776 expression levels in primary AML cells. The *GAPDH* gene was used as an internal control.
777 Relative gene expression levels were calculated as $2^{-\Delta Ct}$. (**M**) Schematic diagram showing
778 primary AML cells killed by CAR-NK cells *in vitro*. Each group of NK cells was co-cultured
779 with primary AML cells for 20 hours at indicated E:T ratios (n = 4 per group). (**N-P**) Specific
780 cytotoxicity of CAR-NK cells derived from UCB-NK against primary AML cells from three
781 patients (Patient #1: N, Patient #2: O, Patient #3: P). Statistical analysis: one-way ANOVA. NS:
782 not significant; *$P < 0.05$, **$P < 0.01$, ***$P < 0.001$.

Fig. 2

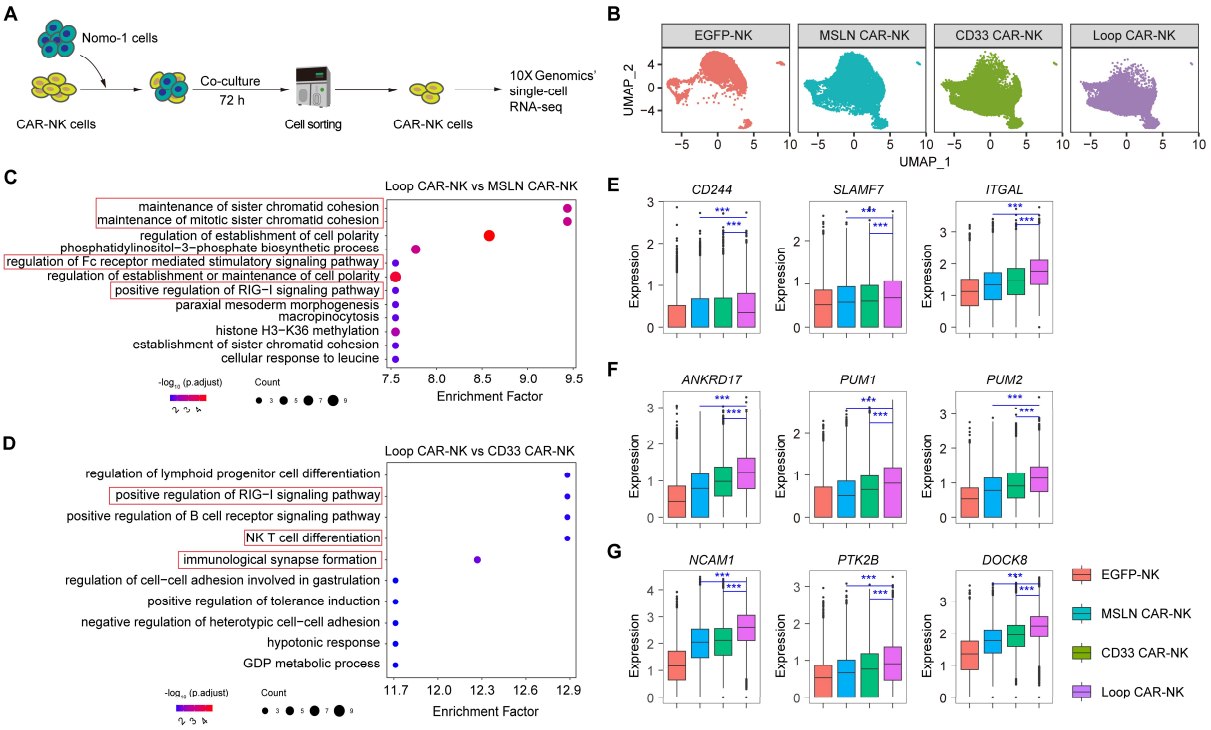

Fig. 2. Molecular characterization of Loop CAR-NK cells. (**A**) Schematic diagram of sorting CAR-NK cells for 10× Genomics' single-cell RNA-seq assay. CAR-NK cells were incubated with Nomo-1 cells (E:T = 1:1) for 72 h before sorting for RNA-seq. (**B**) UMAP visualization contrasting EGFP-NK, CD33 CAR-NK, MSLN CAR-NK, and Loop CAR-NK cells. EGFP-NK cells were used as control. (**C** and **D**) Gene Ontology (GO) analysis of differentially highly expressed genes in Loop CAR-NK cells compared with MSLN CAR-NK (C) and CD33 CAR-NK (D) cells, respectively. Each data point represented a distinct GO set. The color scale corresponded to $-\log_{10}$ transformed false discovery rate (FDR)– adjusted P values. The size of the dot was the number of genes enriched in one term. The enrichment factor was GeneRatio/BgRatio. (**E-G**) Box plots showed the expression profiles of differentially highly expressed genes related to activation and cytotoxicity of NK cells (E), participating in the RIG-1 signaling pathway (F), and involving in immunological synapse formation (G) in Loop CAR-NK cells compared with CD33 CAR-NK and MSLN CAR-NK cells.

Fig. 3

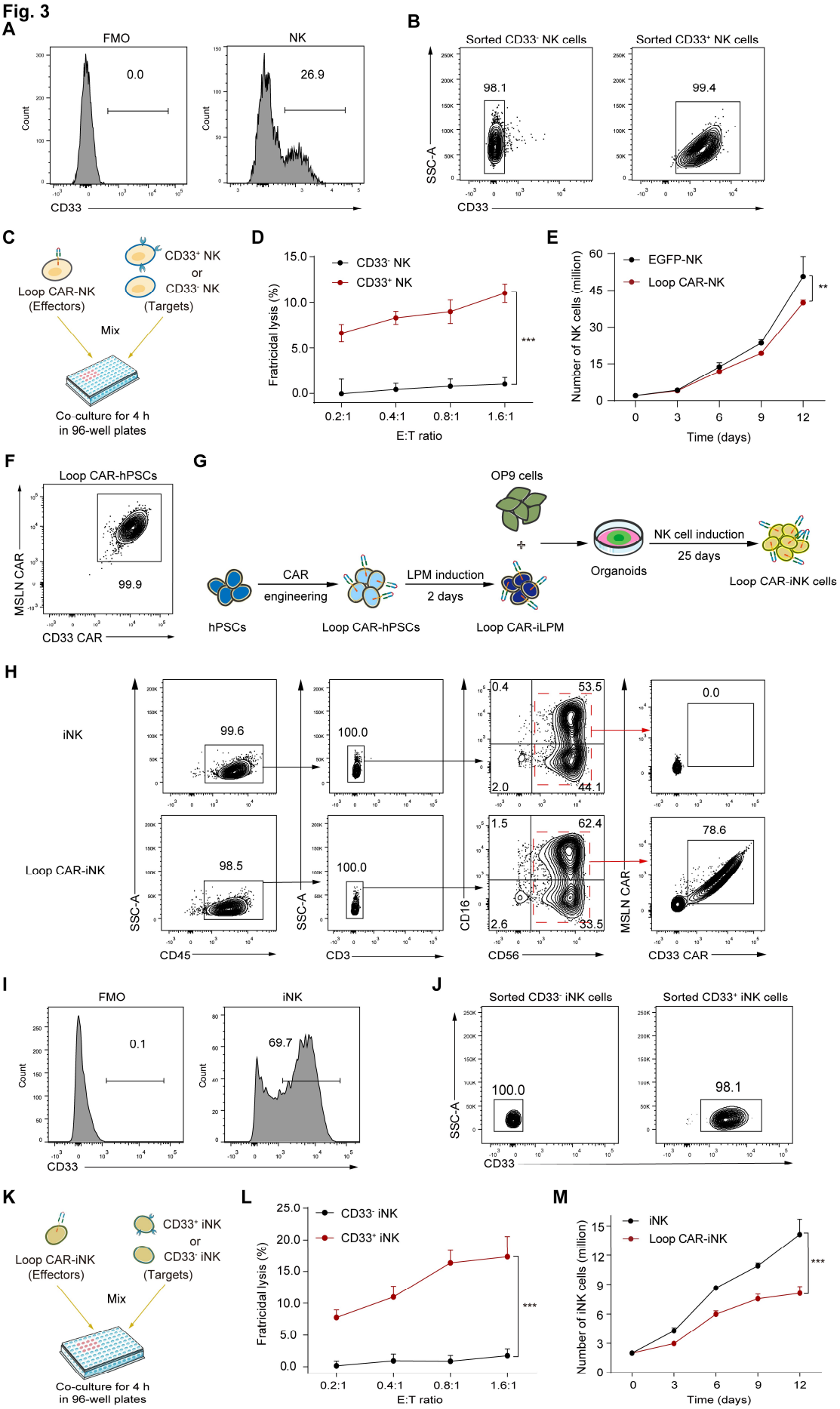
A
FMO
NK
0.0
26.9
Count
CD33
B
Sorted CD33⁻ NK cells
Sorted CD33⁺ NK cells
98.1
99.4
SSC-A
CD33
C
Loop CAR-NK
(Effectors)
CD33⁺ NK
or
CD33⁻ NK
(Targets)
Mix
Co-culture for 4 h
in 96-well plates
D
CD33⁻ NK
CD33⁺ NK
Fratricidal lysis (%)
E:T ratio
0.2:1
0.4:1
0.8:1
1.6:1
***
E
EGFP-NK
Loop CAR-NK
Number of NK cells (million)
Time (days)
**
F
Loop CAR-hPSCs
MSLN CAR
CD33 CAR
99.9
G
OP9 cells
hPSCs
CAR
engineering
Loop CAR-hPSCs
LPM induction
2 days
Loop CAR-iLPM
Organoids
NK cell induction
25 days
Loop CAR-iNK cells
H
iNK
Loop CAR-iNK
99.6
100.0
0.4
53.5
2.0
44.1
0.0
98.5
100.0
1.5
62.4
2.6
33.5
78.6
SSC-A
CD45
CD3
CD16
CD56
MSLN CAR
CD33 CAR
I
FMO
iNK
0.1
69.7
Count
CD33
J
Sorted CD33⁻ iNK cells
Sorted CD33⁺ iNK cells
100.0
98.1
SSC-A
CD33
K
Loop CAR-iNK
(Effectors)
CD33⁺ iNK
or
CD33⁻ iNK
(Targets)
Mix
Co-culture for 4 h
in 96-well plates
L
CD33⁻ iNK
CD33⁺ iNK
Fratricidal lysis (%)
E:T ratio
0.2:1
0.4:1
0.8:1
1.6:1
***
M
iNK
Loop CAR-iNK
Number of iNK cells (million)
Time (days)
***

797

Fig. 3. Expression of CD33 in NK or iNK cells led to fratricide and precluded expansion of Loop CAR-NK or Loop CAR-iNK cells. (**A**) Flow cytometry histograms showing the expression of CD33 in UCB-NK cells. (**B**) Representative FACS plots showing the purity of sorted $CD33^-$ and $CD33^+$ NK cells. (**C**) Schematic diagram of measuring the cytotoxicity of Loop CAR-NK cells against $CD33^+$/$CD33^-$ NK cells *in vitro*. The sorted NK cells were co-cultured with Loop CAR-NK cells for 4 h. (**D**) Statistics of the fratricidal lysis of CAR-NK cells Loop CAR-NK cells (Effectors, E) against $CD33^+$ and $CD33^-$ NK cells (Targets, T) at the indicated E:T ratios (n = 4 per group). (**E**) Statistical analysis of the cell number for EGFP-NK and Loop CAR-NK cells at indicated time points. An equal number of EGFP-NK and Loop CAR-NK cells were sorted for expansion *in vitro* (n = 3 per group). (**F**) Flow cytometric analysis of Loop-CAR expression in Loop CAR-hPSCs. (**G**) Schematic diagram of Loop CAR-iNK cells generated from Loop CAR-hPSCs. (**H**) Immunophenotypes ($CD45^+CD3^-CD56^+CD16^{+/-}$) and Loop-CAR expression (CD33 CAR^+MSLN CAR^+) of Loop-CAR-iNK cells. (**I**) Flow cytometry histograms showing the expression levels of CD33 in iNK cells derived from hPSCs. (**J**) Representative FACS plots showing the the purity of sorted $CD33^-$ and $CD33^+$ iNK cells. (**K**) Schematic diagram of measuring the cytotoxicity of Loop CAR-iNK cells against $CD33^+$ and $CD33^-$ iNK cells *in vitro*. (**L**) Statistics of fratricidal lysis of Loop CAR-iNK cells (Effectors, E) against $CD33^+$ and $CD33^-$ iNK cells (Targets, T) at indicated E:T ratios (n = 4 per group). (**M**) Statistical analysis of the cell number for iNK and Loop CAR-iNK cells at indicated time points (n = 3 per group). An equal number of iNK and Loop CAR-iNK cells were started for culture. Data represent the mean ± SEM. Statistics analysis: one-way ANOVA test (D, L) and two-way ANOVA test (E, M). NS: not significant; $^{**}P < 0.01$, $^{***}P < 0.001$.

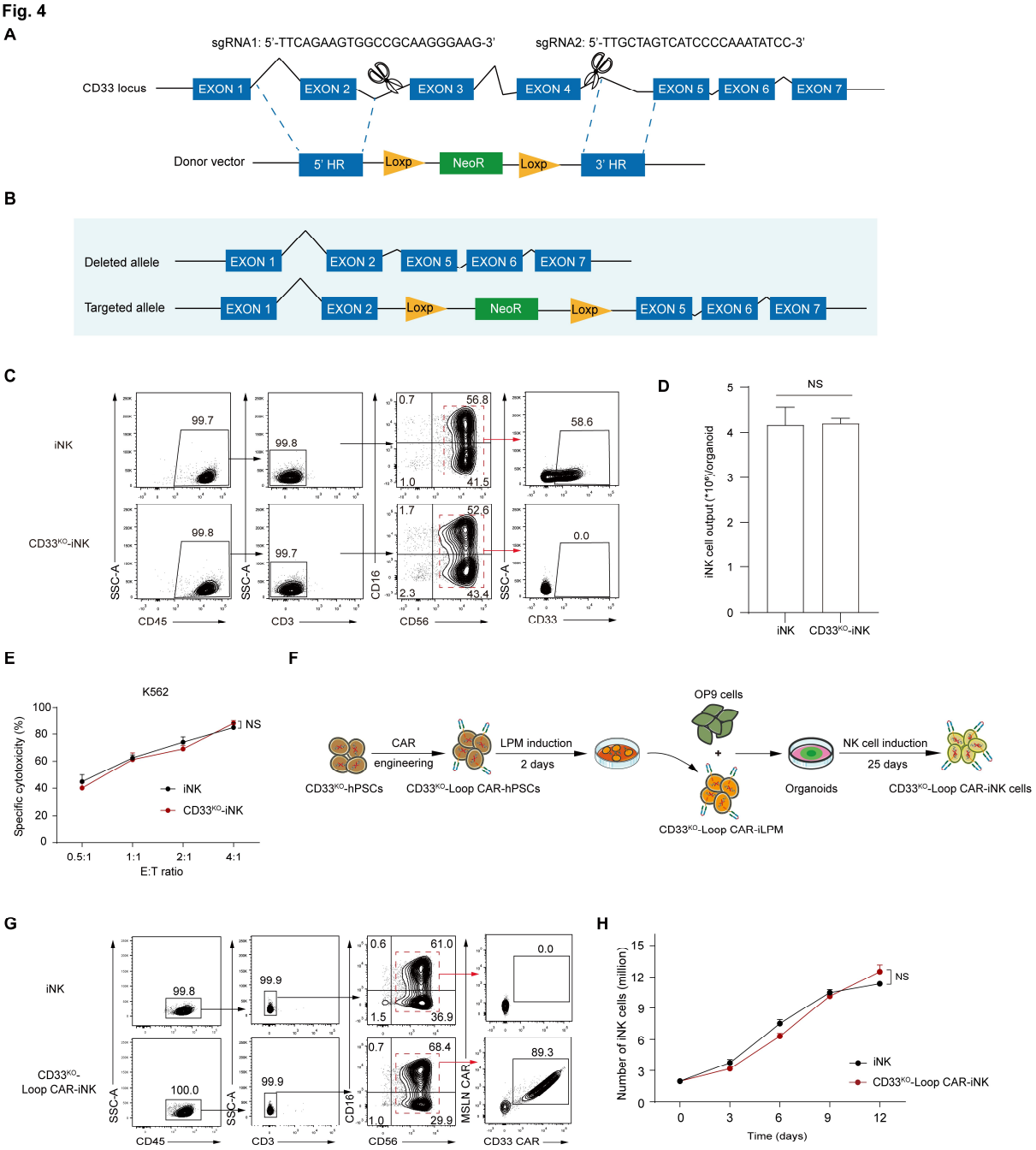

Fig. 4. Inactivation of CD33 restored the expansion of Loop CAR-iNK cells. (**A**) Schematic diagram of CRISPR/Cas12i-targeted CD33 gene strategy. sgRNA: single guide RNA; HR: homologous region; NeoR: neomycin resistance gene. (**B**) Schematic diagram showing the genotype of the established CD33^{KO}-hPSCs. (**C**) Flow cytometric analysis of iNK and CD33^{KO}-iNK cells. (**D**) Statistics of the yields of iNK and CD33^{KO}-iNK cell (Day 27) induced from hPSCs and CD33^{KO}-hPSCs (n = 3 repeats). (**E**) Statistics of cytotoxicity of iNK and CD33^{KO}-iNK cells (Effectors, E) against K562 cells (Targets, T) at the indicated E:T ratios (n

829 = 4 per group). (**F**) Schematic diagram of $CD33^{KO}$-Loop CAR-iNK cells induced from
830 $CD33^{KO}$-Loop CAR-hPSCs. (**G**) Immunophenotypes ($CD45^{+}CD3^{-}CD56^{+}CD16^{+/-}$) and Loop-
831 CAR expression in iNK and $CD33^{KO}$-Loop CAR-iNK cells. (**H**) Statistical analysis of the cell
832 number for iNK and $CD33^{KO}$-Loop CAR-iNK cells at indicated time points. An equal number
833 of iNK and Loop CAR-iNK cells were started for culture (n = 3 repeats). Data represent the
834 mean ± SEM. Statistics analysis: two-tailed Student's t test (D), one-way ANOVA test (E) and
835 two-way ANOVA test (H). NS: not significant.

Fig. 5

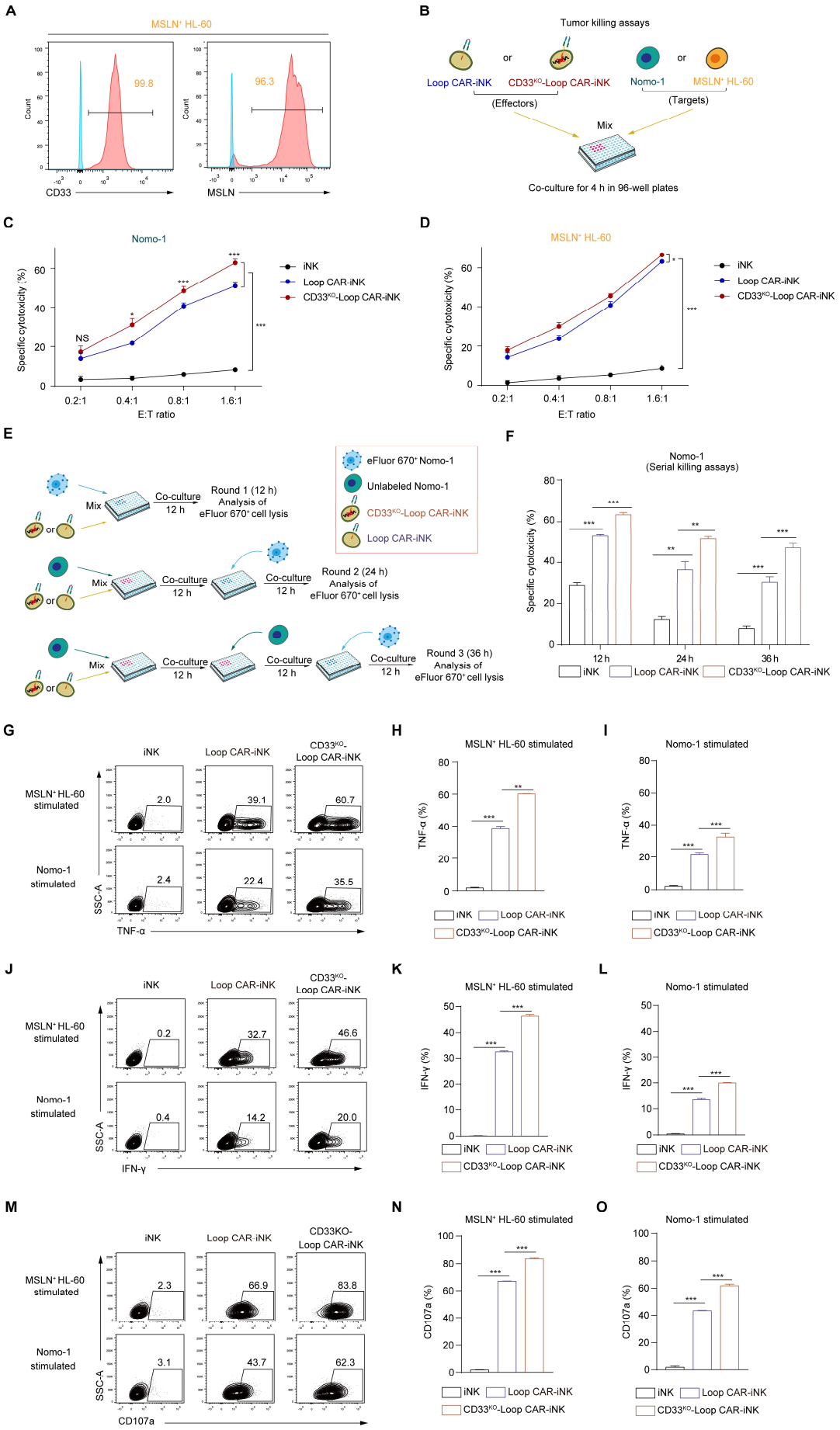
A
MSLN⁺ HL-60
99.8
96.3
Count
CD33
MSLN
B
Tumor killing assays
Loop CAR-iNK
or
CD33KO-Loop CAR-iNK
Nomo-1
MSLN⁺ HL-60
(Effectors)
(Targets)
Mix
Co-culture for 4 h in 96-well plates
C
Nomo-1
Specific cytotoxicity (%)
E:T ratio
0.2:1
0.4:1
0.8:1
1.6:1
NS
iNK
Loop CAR-iNK
CD33KO-Loop CAR-iNK
D
MSLN⁺ HL-60
E
eFluor 670⁺ Nomo-1
Unlabeled Nomo-1
CD33KO-Loop CAR-iNK
Loop CAR-iNK
Mix
Co-culture
12 h
Round 1 (12 h)
Analysis of
eFluor 670⁺ cell lysis
Round 2 (24 h)
Round 3 (36 h)
F
Nomo-1
(Serial killing assays)
12 h
24 h
36 h
G
iNK
Loop CAR-iNK
CD33KO-
Loop CAR-iNK
MSLN⁺ HL-60
stimulated
Nomo-1
stimulated
2.0
39.1
60.7
2.4
22.4
35.5
SSC-A
TNF-α
H
MSLN⁺ HL-60 stimulated
TNF-α (%)
I
Nomo-1 stimulated
J
0.2
32.7
46.6
0.4
14.2
20.0
IFN-γ
K
IFN-γ (%)
L
M
2.3
66.9
83.8
3.1
43.7
62.3
CD107a
N
CD107a (%)
O

836

Fig. 5. CD33^{KO}-Loop CAR-iNK cells exhibited superior tumor-killing abilities than Loop CAR-iNK cells. (**A**) Flow cytometry histograms showing the expression of CD33 and MSLN in HL-60 cells engineered with MSLN (MSLN^{+}HL-60). (**B**) Schematic diagram showing Nomo-1 or MSLN^{+} HL-60 cells killed by Loop CAR-iNK or CD33^{KO}-Loop-CAR-iNK cells *in vitro*. (**C** and **D**) Statistics of specific cytotoxicities analysis of iNK, Loop CAR-iNK and CD33^{KO}-Loop CAR-iNK cells (Effectors, E) against Nomo-1 (C) and CD33^{+}MSLN^{+} HL-60 cells (D) (Targets, T) at the indicated E:T ratios (n = 4 per group). (**E**) Schematic diagram of the serial killing assays of iNK, Loop CAR-iNK, and CD33^{KO}-Loop CAR-iNK cells against Nomo-1 cells. Each group of iNK cells was co-cultured with Nomo-1 cells for 12 h per round at an E:T ratio of 1:1. The fresh Nomo-1 cells were added to the NK cell residues and incubated for every other 12 h. The lysis of Cell Proliferation Dye eFluor 670-labeled (eFluor 670^{+}) Nomo-1 cells in each round represented the cytotoxicity. (**F**) Statistics of specific cytotoxicity of iNK, Loop CAR-iNK, and CD33^{KO}-Loop CAR-iNK cells in serial killing assays (n = 4 per group). (**G**, **J**, **M**) Representative flow cytometry plots showing the expression of TNF-α (G), IFN-γ (J), and CD107a (M) in each group of iNK cells stimulated by MLSN^{+} HL-60 and Nomo-1 cells. (**H** and **I**) Statistical analysis of the expression levels of TNF-α (n = 3 repeats). (**K** and **L**) Statistical analysis of the expression levels of IFN-γ (n = 3 repeats). (**N** and **O**) Statistical analysis of the expression levels of CD107a (n = 3 repeats). Data represent the mean ± SEM. Statistics analysis: one-way ANOVA test. NS: not significant; *$P < 0.05$, **$P < 0.01$, ***$P < 0.001$.

Fig. 6

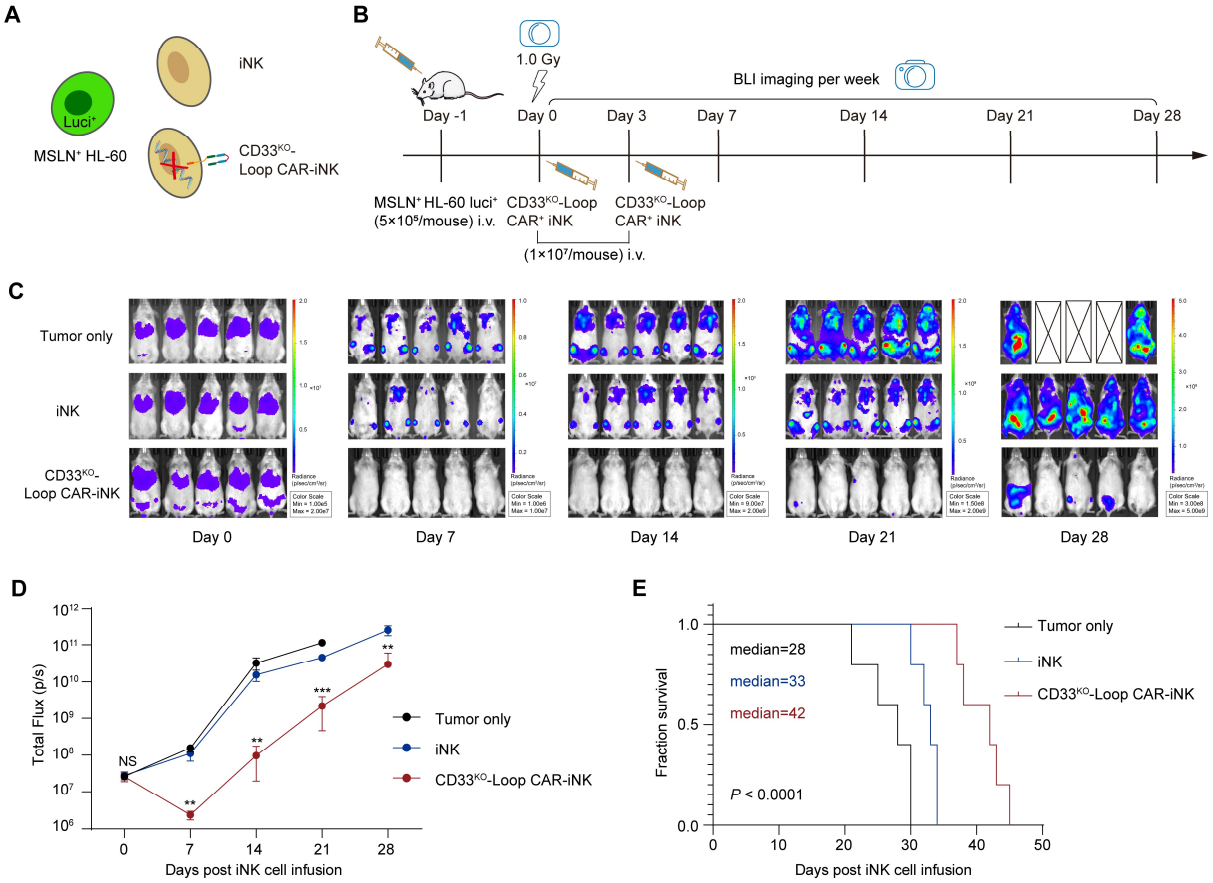

857

858 **Fig. 6. CD33^{KO}-Loop CAR-iNK cells efficiently suppressed tumor progression *in vivo*.** (**A**)
859 Schematic diagram of the tumor cells and therapeutic cells used for *in vivo* assay. (**B**) Schematic
860 diagram of *in vivo* studies. Luciferase-expressing (luci^{+}) MSLN^{+} HL-60 cells were used to
861 generate mouse xenograft models (5 × 10^5 cells/mouse, i.v.). Two doses of CD33^{KO}-Loop
862 CAR-iNK cells (1× 10^7 cells/mouse per dose) were injected into tumor-bearing mice for
863 therapy. (**C**) Bioluminescence imaging (BLI) of xenograft models of each group (n = 5 per
864 group). (**D**) Statistics of each group's total flux (p/s) (CD33^{KO}-Loop CAR-iNK vs. iNK).
865 Statistics analysis: two-tailed Student's t-test. NS: not significant; $^{**}P < 0.01$, $^{***}P < 0.001$.
866 (**E**) Kaplan-Meier survival curves of the experimental groups. Statistics analysis: two-tailed
867 log-rank test. Tumor only vs. iNK, $^{**}P < 0.01$, CD33^{KO}-Loop CAR-iNK vs. iNK, $^{**}P < 0.01$.
868

869 **Supplementary Materials**

Fig. S1

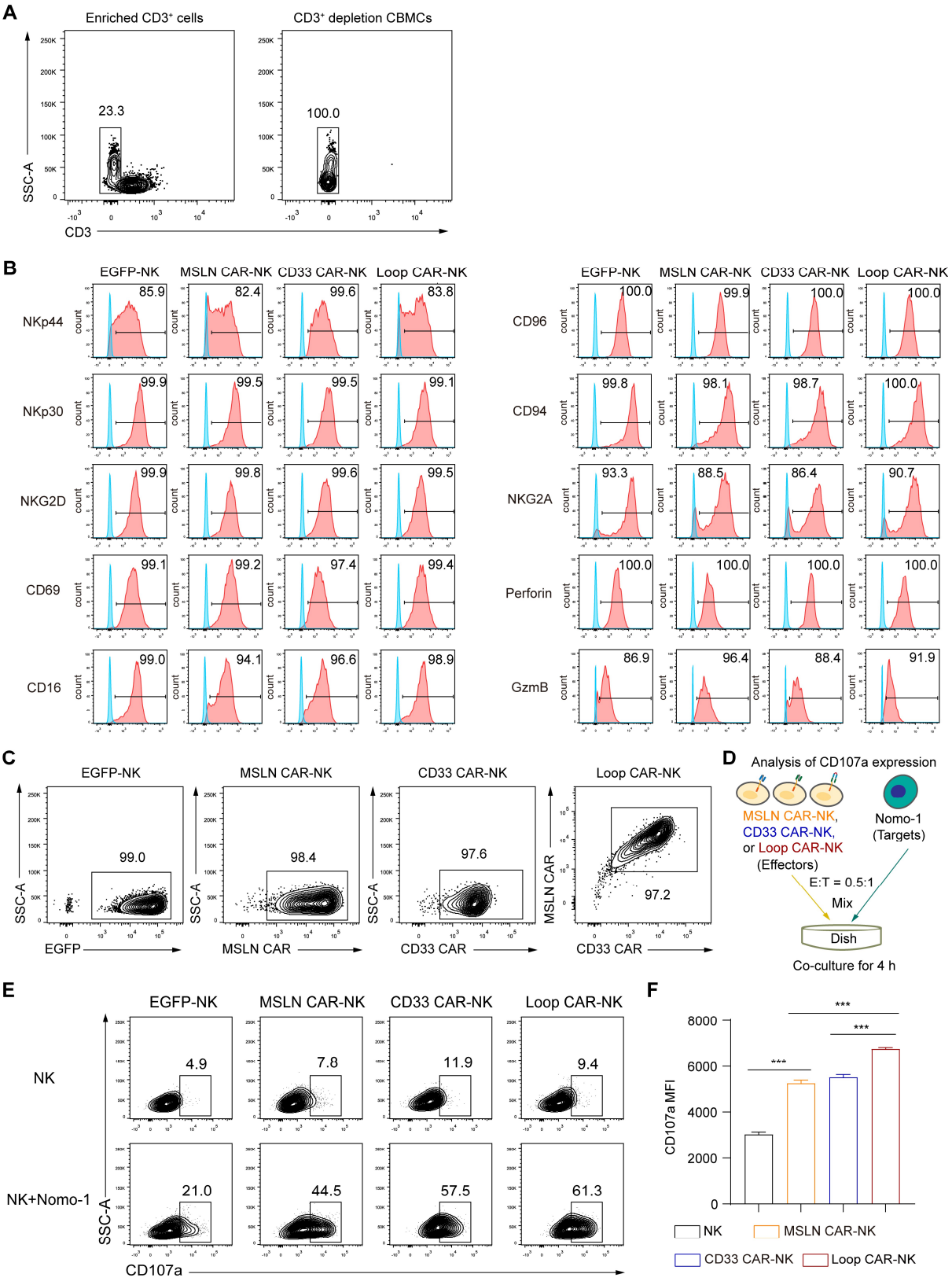

870

871 **Fig. S1. Phenotypes and effector function of Loop CAR-NK cells.** (A) Flow cytometric

analysis of the T cells ($CD3^+$) residual in UCBMCs after $CD3^+$ cells depletion on day -6. (B) Flow cytometry histograms showing the expression of typical NK cell receptors (NKp44, NKp30, NKG2D, CD69, CD16, CD96, CD94, and NKG2A) and cytotoxic granules (Perforin and GzmB) in respective NK cells. Control histograms represent FMO control. (C) The analysis of sorting purity for $CD3^-CD56^+EGFP^+$ (EGFP-NK) and $CD3^-CD56^+CAR^+$ (CAR-NK) cells post 24 h culturing. (D) Experimental design of the analysis of CD107a expression. EGFP-NK and CAR-NK cells were stimulated at an E:T ratio of 0.5:1 for 4 h. (E) Representative flow cytometry plots showing the expression of CD107a in EGFP-NK and CAR-NK cells in response to Nomo-1 cells. (F) Statistic analysis of the mean fluorescence intensity (MFI) of CD107a in (E), n = 3 repeats. Statistical analysis: one-way ANOVA, ***P < 0.001.

Fig. S2

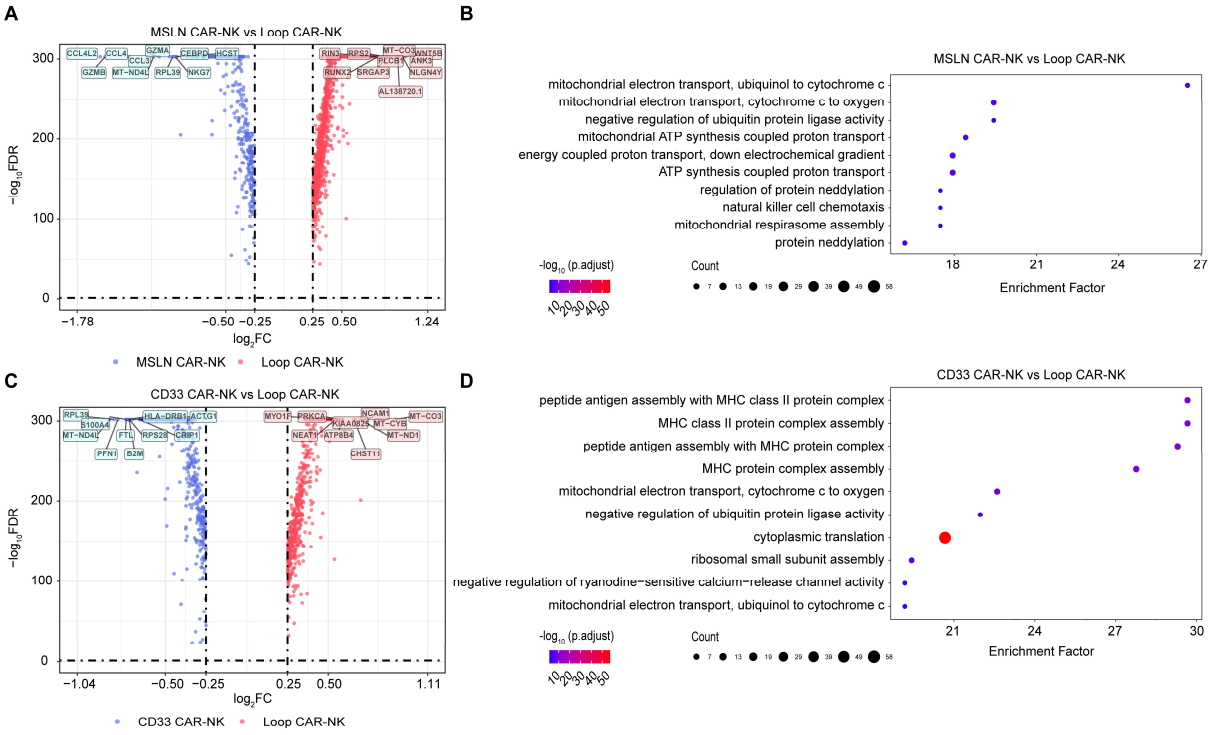

Fig. S2. Differentially expressed genes of Loop CAR-NK cells compared with CD33 CAR-NK and MSLN CAR-NK cells. (A) Volcano plot of differentially expressed genes between Loop CAR-NK and MSLN CAR-NK cells. (B) GO analysis of differentially down-regulated

genes in Loop CAR-NK cells compared with MSLN CAR-NK. Each data point represents a distinct GO set. Color scale corresponds to −log10 FDR (adjusted P values). Dot size was the number of genes enriched in one term. Enrichment Factor was the GeneRatio/BgRatio. (C) Volcano plot of differentially expressed genes between Loop CAR-NK and CD33 CAR-NK cells. (D) GO analysis of differentially down-regulated genes in Loop CAR-NK cells compared with CD33 CAR-NK cells. Each data point represents a distinct GO set. Color scale corresponds to −log10 FDR (adjusted P values). Dot size was the number of genes enriched in one term. Enrichment Factor was the GeneRatio/BgRatio.

Fig. S3

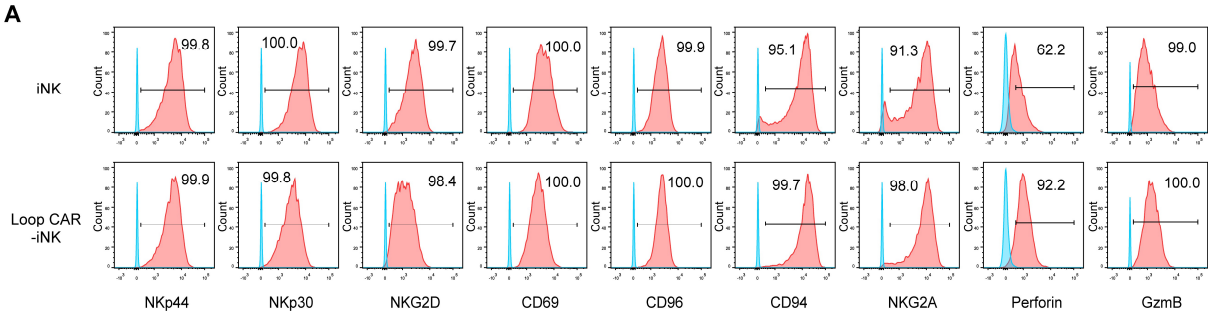

Fig. S3. Analysis of typical NK molecules of Loop CAR-iNK cells. (A) Flow cytometry histograms showing the expression of typical NK cell receptors (NKp44, NKp30, NKG2D, CD69, CD96, CD94, and NKG2A) and cytotoxic granules (Perforin and GzmB) in respective iNK cells. Control histograms represent FMO control.

Fig. S4

A

Primer No.	Forword primer sequence	Reverse primer sequence
1	5'-TCCCAGTAGGAACAACTGCTCCCTGAGCATCGTAGACGCC-3'	5'-TAAATGTTCAAGATGATGGATATGCTATTACCCTGATCTG-3'
2	5'-TCCCAGTAGGAACAACTGCTCCCTGAGCATCGTAGACGCC-3'	5'-GATGGATTGCACGCAGGTTC-3'
3	5'-CATGAGGCTAGAAAGGAAATTGGAACTTAAAGAGGCAGTG-3'	5'-GCAGCTGACAACCAGGAGAAGATC-3'
4	5'-CTCGGTGCTCATAATCACCCCACGG-3'	5'-CTATTCATCTGACAAGTGATTCATATCCAGAACATACGAG-3'

B

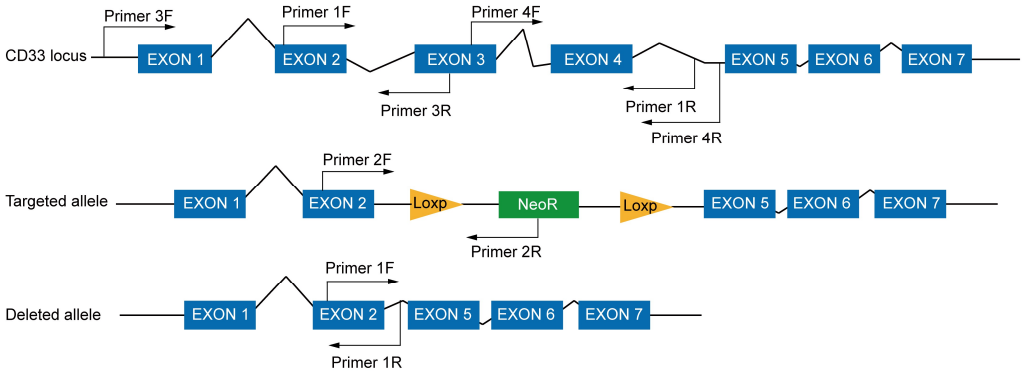

C

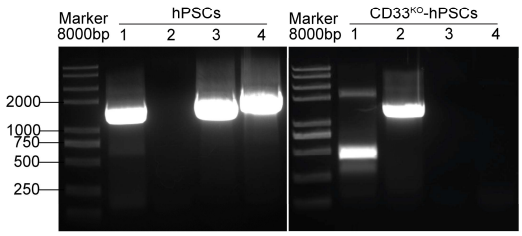

D

Primer NO.	hPSCs	CD33^{KO}-hPSCs
1	1241 bp	2124 bp, 302 bp
2	\	1282 bp
3	1437 bp	\
4	1673 bp	\

E

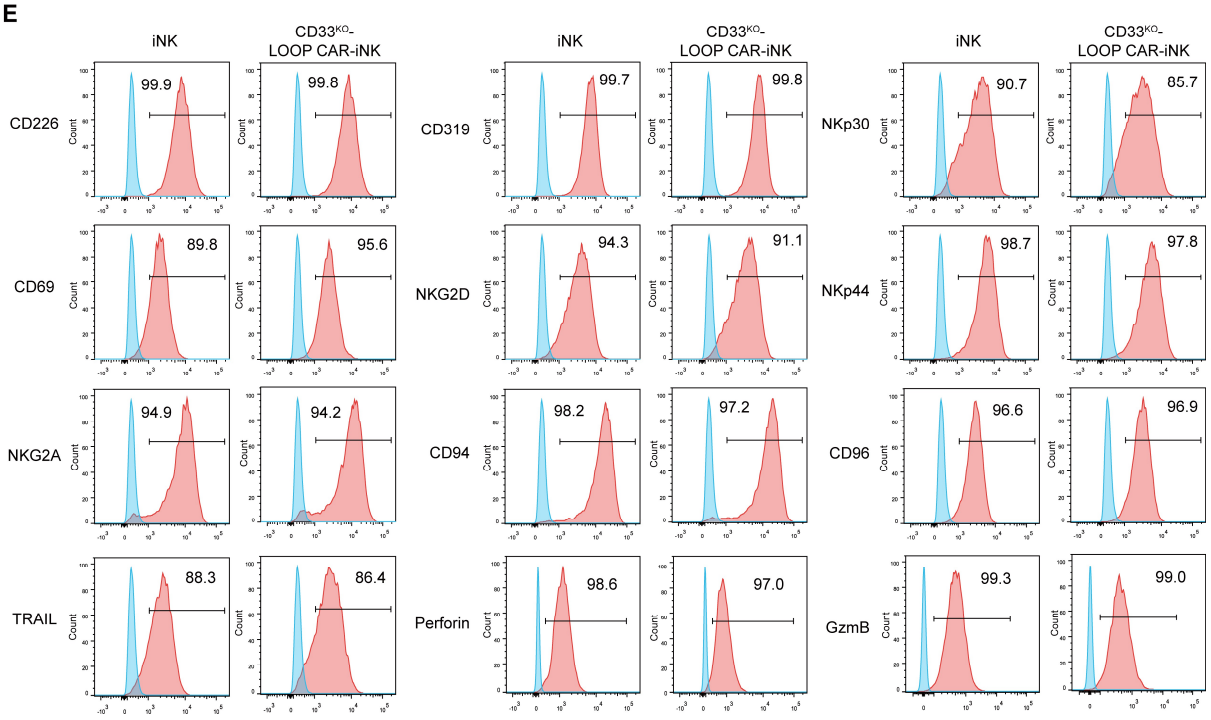

Fig. S4. Identification of CD33 genotypes of CD33^{KO}-hPSCs and molecular features of

902 **CD33^{KO}-Loop CAR-iNK cells.** (A) The sequences of four pairs of primers used for
903 genotyping CD33 knock-out PSC clones. (B) Schematic diagram showing the location of
904 primer pairs used for identifying CD33 genotypes. (C, D) PCR amplification results of each
905 fragment using the indicated primer pairs. (E) Flow cytometry analysis of typical NK cell
906 receptors (CD226, CD319, NKp30, CD69, NKG2D, NKp44, NKG2A, CD94, CD96, TARIL)
907 and cytotoxic granules (Perforin and GzmB) in respective iNK cells. Control histograms
908 represent FMO control.

Primer name	Primer sequence (5'→3')
GAPDH-F	CAAGAAGTGGGAGCTGGAAG
GAPDH-R	GTCTCCAGGGACGTCACATT
MSLN-F	ACCCAGAAGACTGTGGATGG
MSLN-R	TGCTGTAGCCAAATTCGTTG

909 **Table S1. Primer sequences for real-time quantitative PCR of selected genes.**